

Unlimited Release
Printed June 1991

THE DEPTH OF THE OIL/BRINE INTERFACE
AND CRUDE OIL LEAKS IN SPR CAVERNS

Grant S. Heffelfinger
Underground Storage Technology Division 6257
Sandia National Laboratories
Albuquerque, New Mexico 87185

ABSTRACT

Monitoring **wellhead** pressure evolution is the best method of detecting crude oil leaks in SPR caverns while oil/brine interface depth measurements provide additional insight. However, to fully utilize the information provided by these interface depth measurements, a thorough understanding of how the interface movement corresponds to cavern phenomena, such as salt creep, crude oil leakage, and temperature equilibration, as well as to **wellhead** pressure, is required. The time evolution of the oil/brine interface depth is a function of several opposing factors. Cavern closure due to salt creep and crude oil leakage, if present, move the interface upward. Brine removal and temperature equilibration of the oil/brine system move the interface downward. Therefore, the relative magnitudes of these factors determine the net direction of interface movement. Using a mass balance on the cavern fluids, coupled with a simplified salt creep model for closure in SPR caverns, the movement of the oil/brine interface has been predicted for varying cavern configurations, including both right-cylindrical and carrot-shaped caverns. Three different cavern depths and operating pressures have been investigated. In addition, the caverns were investigated at four different points in time, allowing for varying extents of temperature equilibration. Time dependent interface depth changes of a few inches to a few feet were found to be characteristic of the range of cases studied.

ACKNOWLEDGEMENTS

The author thanks Jim Todd for many technical discussions which have contributed to the development of the simplified SPR creep model used in this and other work as well as to the interpretation of the cavern phenomena to which this model has been applied. Jim Linn suggested several changes to this work which enhanced its usefulness.

INTRODUCTION

The ability to detect leaks in oil storage caverns in the U.S. Department of Energy's Strategic Petroleum Reserve (SPR) is important. These caverns, leached in Gulf Coast salt domes, are nominally some 2000 ft underground, thus affording the cavern engineer very little means of direct observation to detect leaks. The cavern engineer does have daily readings of cavern **wellhead** pressure which, combined with a data base of such readings, can give a good indication of the existence of leaks as well as their approximate size (Biringer 1987).

Measurement of the oil/brine interface depth in SPR caverns provides additional information concerning leaks. This information is especially useful in cases when the **wellhead** pressure data, $P(t)$, is not definitive or when the cavern has had a series of significant interruptions such as the addition or removal of oil. However, several opposing time-dependent phenomena determine the direction of interface movement. This, coupled with the fact that most caverns are relatively frequently interrupted, makes using interface depth readings to detect leaks a difficult procedure. Furthermore, the exact location of the interface is difficult to determine. Not only are interface depth measurements normally accurate only to 1 or 2 inches, but the interface depth itself can be difficult to define. This is a result of a sludge layer which forms at the oil/brine interface, the thickness and consistency of which depends on the oil composition and cavern residence time. Monitoring **wellhead** pressure data is therefore the preferred means for detecting leaks in SPR caverns, while interface depth measurements, if properly understood, can supplement this information. This document provides the technical basis for interpreting interface measurements.

INTERFACE MOVEMENT AND RELATED PARAMETERS

Leaks in solution-mined caverns generally occur in or near the casing seat, no leaks have been confirmed in the bottom of caverns. Thus cavern leaks would be crude oil leaks, which result in an upward movement of the oil/brine interface. An upward interface movement also results naturally from cavern creep closure due to the fact that the volume lost by creep closure is concentrated in the brine (bottom) region of the cavern (Heffelfinger, 1991) and that the brine is less compressible than oil. On the other hand, removing brine results in a downward movement of the interface. Similarly, since the cavern is nominally filled with approximately 294 K (70°F) crude oil, the greater temperature of the salt dome heats the oil, expanding it and moving the interface downward with time. Thus SPR caverns are dynamic systems, with interface depth controlled by the relative rates of cavern creep, fluid reduction, whether via crude oil leakage or brine removal, and temperature equilibration. Therefore the size of a leak (bbl/day) or the brine removal rate (bbl/day) relative to the volume loss due to creep closure (bbl/day) determines the direction of the interface movement. The

magnitude of this effect depends upon the cavern's age since the creep rate, and thermal effects, change with time.

In addition to the creep closure, fluid removal rates, and thermal equilibration, gas intrusions from the salt, cavern depth, shape, and **wellhead** pressure affect the movement of the interface. Cavern depth and **wellhead** pressure have a direct effect on the creep rate while cavern shape affects the relationship between the interface depth and the relative amounts of crude oil and brine due to the geometric link between cavern shape and volume distribution.

Interface depth and leak rate have been related to cavern shape, depth, time since fill, and **wellhead** pressure in the following manner. Using a simplified creep model (Heffelfinger 1991), modified to include the cavern's thermal equilibration (discussed in Appendix A) and its elastic response to pressure changes (discussed in Appendix B), caverns of two different shapes, right-circular cylindrical and carrot-shaped, were **modelled** at three different depths, 1500 - 3500 ft, 2000 - 4000 ft, and 2500 - 4500 ft, and at one operating pressure, 600 psia.

The time since fill for these caverns was taken to be 10 years. This cavern age implies that the oil contained in such caverns have been allowed to thermally equilibrate without interruption for 10 years. Due to extraneous operational constraints, SPR cavern's are often frequently interrupted with oil and/or brine removals and additions thus this concept of the oil temperature profile as related to cavern age is an approximation.

In addition, at one depth, 2000 - 4000 ft, three additional times since fill: 1, 5, and 20 years, and two additional **wellhead** pressures, 900 and 1200 psia, were investigated. Initial interface depths were taken to be 250 ft from the bottom of the cavern for all cases.

This model treats leak rate as independent of cavern pressure. Although this is not the case for real SPR caverns, the intent of this work is to relate the combined effects of the rates of creep closure, volume loss, and thermal equilibration, to interface movement rather than to address the relationship between cavern operating pressure and leak rate. The temperature profile of the salt is taken to be linear with depth and time invariant while that of the oil varies not with depth but with time according to Tomasko's (Tomasko, 1985) calculations for SPR caverns. The oil and salt temperature models are discussed further in Appendix A. Finally, this simplified SPR cavern model does not consider any intrusions of naturally **occurring** gas from the surrounding salt. (This assumption is justified since only a few of the 64 SPR solution-mined caverns have had measurable gas intrusion effects).

The carrot-shaped caverns were designed to represent Phase II SPR caverns while having comparable characteristics to a model cavern, a 2000 ft right-circular cylinder with a radius of 100 ft. Using the rule of thumb that carrot-shaped SPR caverns have a nominal roof radius of 117.5 ft, the floor radius of the carrot-shaped cavern was calculated to be 81.4 ft by setting the volume of the carrot-shaped cavern equal to that of the

model cavern and assuming that the radius varied linearly between the roof and floor. Profiles of both the model right-circular cylindrical cavern as well as the carrot-shaped cavern are shown in Figure 1.

All caverns were **modelled** over 180 days. For the first 90 days, the amount of brine calculated to accommodate the volume loss due to creep closure (Heffelfinger 1991) was removed automatically. The brine was removed at intervals of 30 days to simulate monthly cavern "bleed-downs," used to control **wellhead** pressure and accommodate cavern creep. The difference between this procedure and that actually used by SPR cavern engineers, removing brine when the cavern pressure reaches some predetermined maximum, has been developed in Appendix C. At 90 days, a simulated crude oil "leak" varying from 0 to 100 bbl/day was initiated.

In order to detect a leak the cavern engineer can monitor the evolution of the **wellhead** pressure, $P_w(t)$, and the interface depth, $z_i(t)$. Throughout this work, two additional parameters will be discussed, namely the repressurization ratio, RR, and the change in interface depth, Δz_i . The repressurization ratio is defined by

$$RR = \left| \frac{P_{w \max}(t \geq t_{\text{leak}}) - P_w(t = 0)}{P_{w \max}(t \leq t_{\text{leak}}) - P_w(t = 0)} \right| * 100\% \quad (1)$$

where $P_{w \max}(t \leq t_{\text{leak}})$ is the maximum **wellhead** pressure reached by the cavern prior to the leak, $P_w(t = 0)$ is the initial or baseline **wellhead** pressure, and $P_{w \max}(t \geq t_{\text{leak}})$ is the maximum **wellhead** pressure reached by the cavern after the leak. Notice that the repressurization ratio is the mathematical equivalent of the post-leak slope of the **wellhead** pressure data divided by the pre-leak slope of the **wellhead** pressure data. Notice also that if the leak rate is such that the cavern creep rate is insufficient to repressurize the cavern, the maximum **postleak wellhead** pressure, $P_{w \max}(t \geq t_{\text{leak}})$, will be the **wellhead** pressure at the time of the leak, or equal to $P_w(t = 0)$. If this occurs the numerator of equation 1 will be zero and thus the repressurization ratio, RR, will be zero.

The change in interface depth is defined by

$$\Delta z_i(t) = z_i(t) - z_i(t=0) \quad (2)$$

where $\Delta z_i(t)$ is the change in interface depth as a function of time, $z_i(t)$ is the interface depth as a function of time, and $z_i(t=0)$ is the initial interface depth.

Cavern Cross-Sections

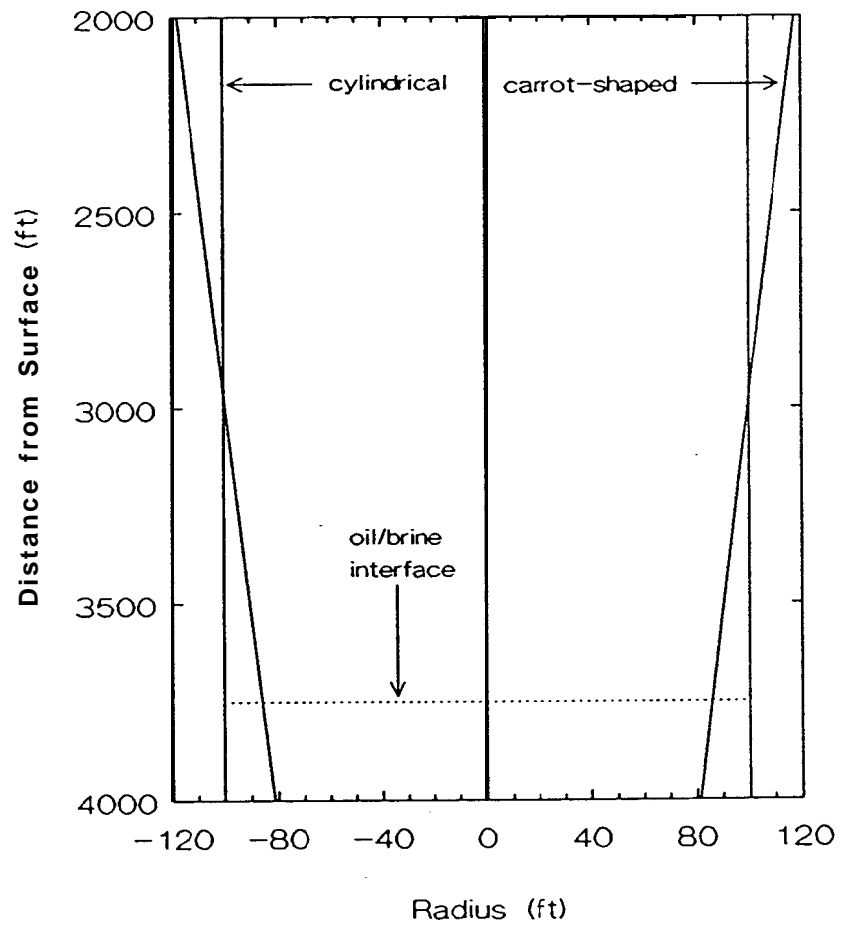


Figure 1. Radius profiles, $r(z)$, the right-circular cylindrical cavern and the carrot-shaped caverns employed in this work.

RESULTS

Repressurization Ratios

An example of **wellhead** pressure evolution and change in interface depth for a 2000 - 4000 ft cavern which has aged 20 years since fill and experiences a leak of 0 bbl/day is shown in Figure 2. This cavern was initialized at a baseline **wellhead** pressure of $P_w = 600$ psia, and with an initial interface depth of $z_i(t=0) = 3750$ ft. The rise in **wellhead** pressure from 0 to 30 days (20 years plus 30 days) for a cavern this age is mostly due to the volume lost to creep closure, and some to thermal heating of the cavern fluids (Appendix A). At 30 days, and at 30 day intervals thereafter, brine is bled from the cavern, resulting in a drop in **wellhead** pressure to its baseline value. Between brine removals, the interface rises, i.e., the change in interface, Δz_i , as a function of time, has a positive slope. When brine is removed at the 30 day intervals, the interface moves downward, as evidenced by the drop in Δz_i . Similar results for the same cavern with a leak rate of 27.9 bbl/day are shown in Figure 3. This leak rate represents a unique value for this cavern: it is the leak rate at which further brine removal is unnecessary to maintain the baseline pressure at 600 psia. That is, if a leak of 27.9 bbl/day occurred from this cavern, the cavern engineer would notice that after the bleed-down at 90 days, the cavern would remain at 600 psia without further intervention. The size of the leak which causes this cavern behavior is unique for each cavern and reflects the creep closure and thermal equilibration rates. This phenomena can be related to cavern depth and operating pressure by examining the relationship between the repressurization ratio, RR, and the leak rate.

In the case of a 0 bbl/day leak, as in Figure 2, the repressurization ratio will be **100%**, i.e., the cavern will fully repressurize after such a leak. For the cavern in Figure 3, the cavern repressurization ratio is 0%. The repressurization ratio is a function not only of leak rate but also creep rate, cavern depth, operating pressure, cavern shape, and extent of thermal equilibration. This can be seen from Figure 4, a plot of the repressurization ratio vs. leak rate for caverns aged 10 years since fill operated at 600 psia for three different depths. Also shown in this figure are the corresponding repressurization ratios for similar caverns which are carrot-shaped. For a given leak rate, the repressurization ratios for carrot-shaped caverns are found to be slightly higher than those of cylindrical caverns.

The effect of thermal equilibration on the relationship between repressurization ratio and leak rate can be seen from Figure 5, a plot of the repressurization ratio/leak rate relationship for a 2000 - 4000 ft cavern at ages: 1, 5, 10, and 20 years since fill. From this data, it can be seen that as cavern's age, they begin to take on the characteristics of shallower caverns. For example, by comparing Figures 4 and 5, we see that the repressurization ratio/leak rate relationship is very similar for 10 year old 1500 - 3500 ft caverns and 20 year old 2000 - 4000 ft caverns. Stated another way, for a given depth, younger caverns repressurize more vigorously than older caverns. This is a

Pressure and Interface Leak Response 2000 - 4000 ft 0 BBL/day

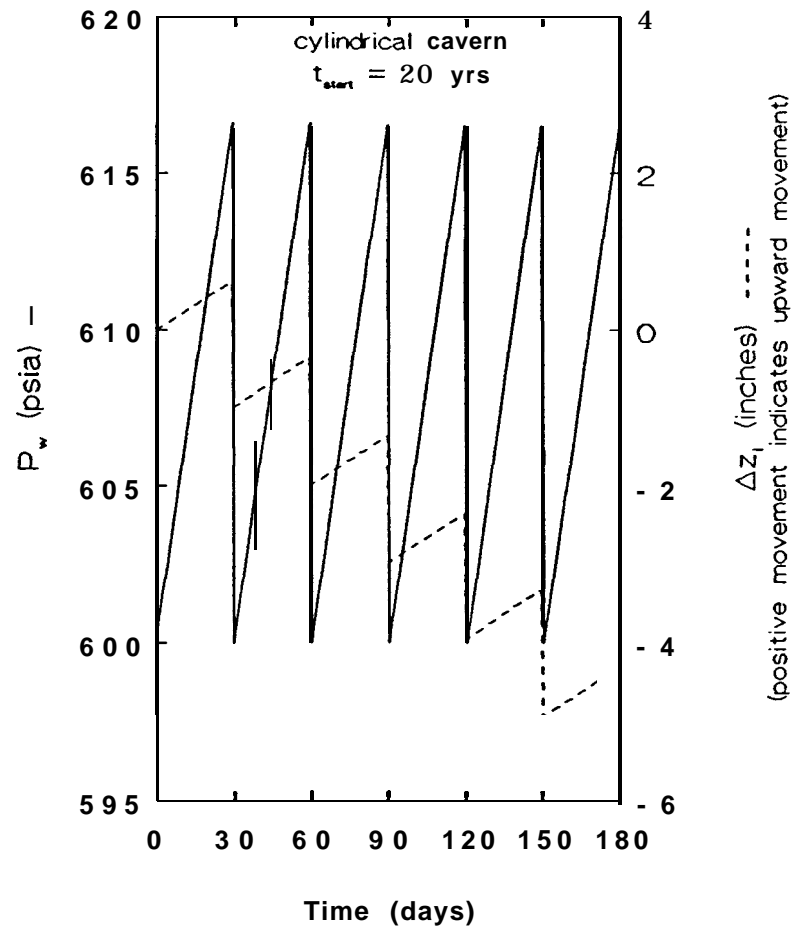


Figure 2. An example of the **wellhead** pressure evolution and the change in interface depth for a 2000 - 4000 ft cavern, 20 years from fill, operated at $P_w = 600$ psia, with a leak of 0 bbl/day.

Pressure and Interface Leak Response 2000 - 4000 ft 27.9 BBL/day

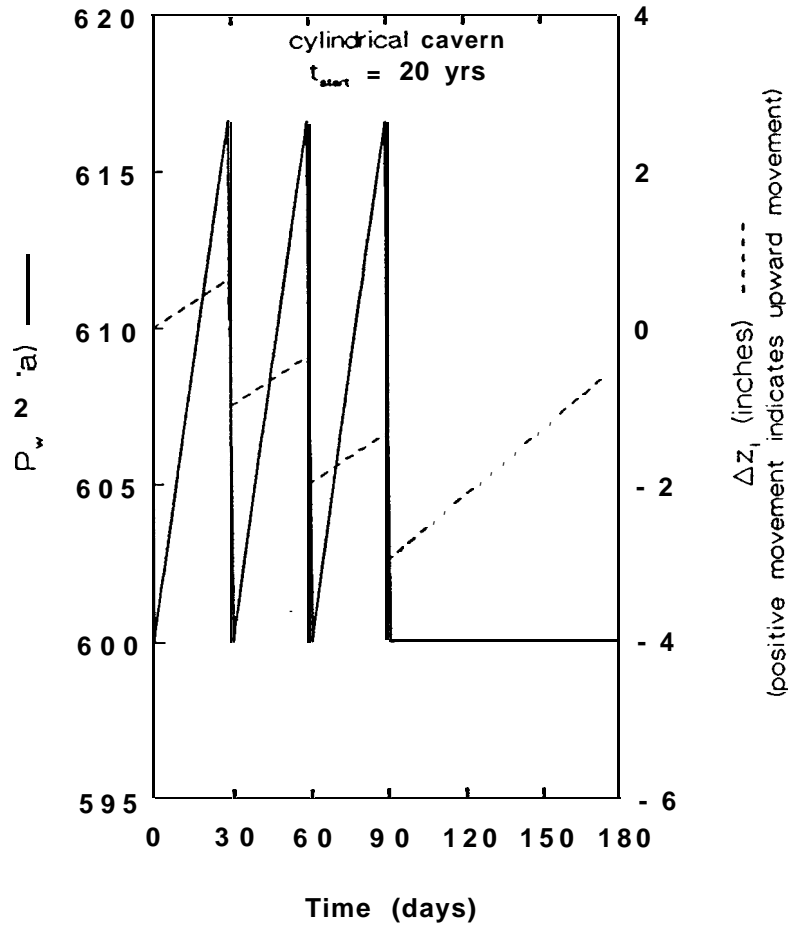


Figure 3. An example of the **wellhead** pressure evolution and the change in interface depth for a 2000 - 4000 ft cavern, 20 years after fill. operated at $P_w = 600$ psia, with a leak of 23.9 bbl/day.

Repressurization Ratios for Caverns Operated at $P_w = 600$ psia

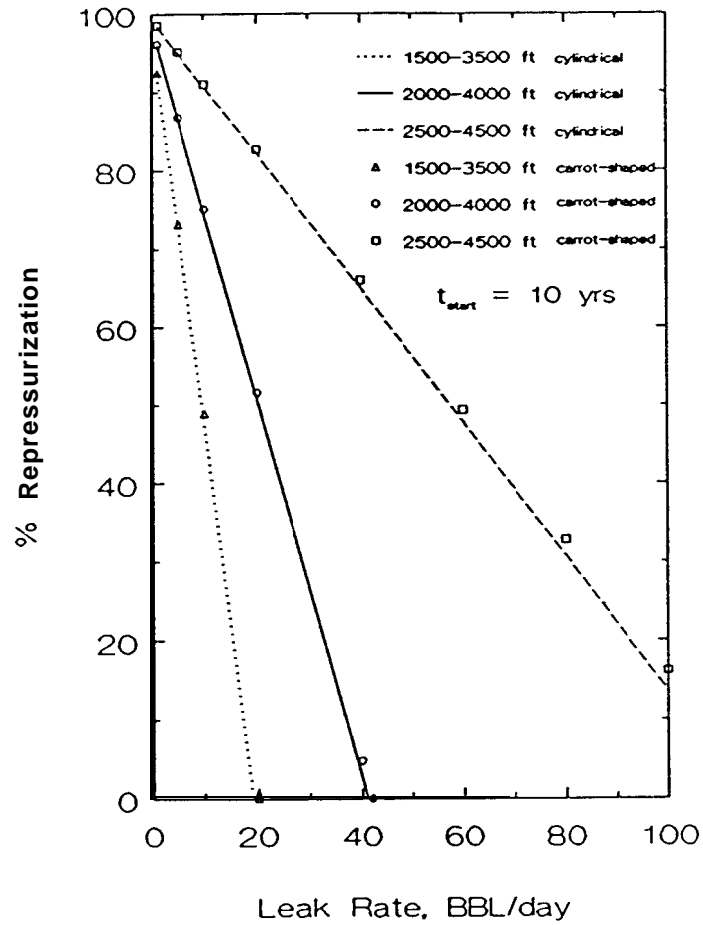


Figure 4. Repressurization ratio vs leak rate for 2000 ft cylindrical and carrot-shaped caverns, 10 years after fill, operated at 600 psia, at three different depths.

Repressurization Ratios for Caverns Operated at $P_w = 600$ psia

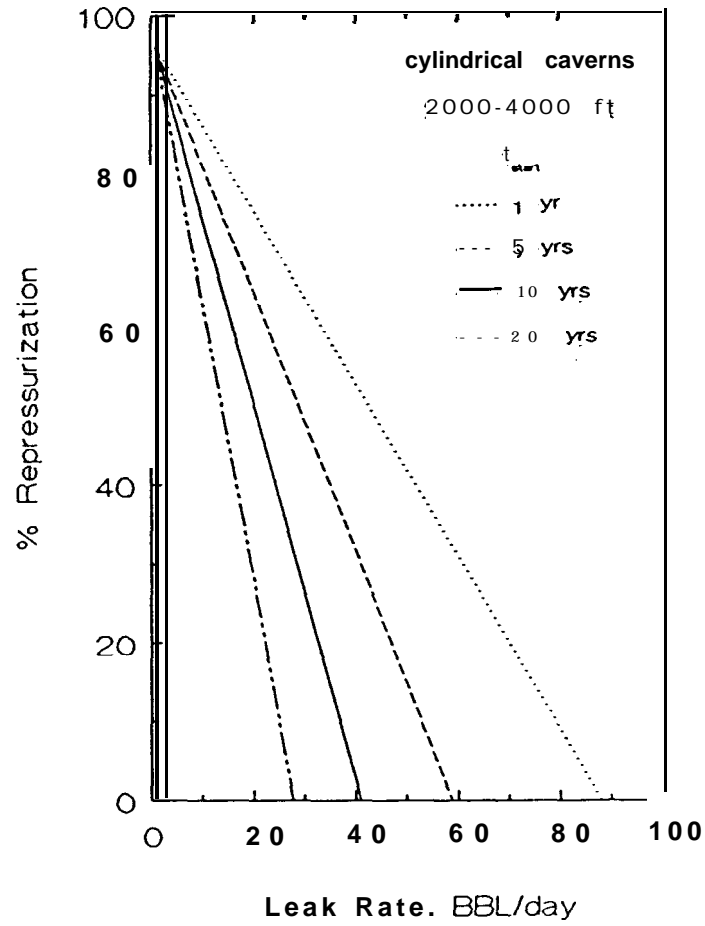


Figure 5. Repressurization ratio vs leak rate for 2000 - 4000 ft cylindrical caverns aged: 1, 5, 10, and 20 years after fill, operated at 600 psia.

direct result of the expansion of the cavern fluids as they increase in temperature and that this increase is more pronounced for younger caverns (see Appendix A).

A similar plot for 2000 - 4000 ft caverns operated at 900 and 1200 psia is presented in Figure 6. From this figure it can be seen that operating the cavern at 900 psia instead of 600 psia has a similar effect on the cavern creep closure rate, and therefore the repressurization-leak rate relationship, as operating a 600 psia cavern at 1500 - 3500 ft instead of 2000 - 4000 ft.

Plots of repressurization ratios for data generated with computer models are useful for understanding cavern behavior. However, it must be emphasized that **wellhead** pressure data from actual caverns is highly scattered. Data reduction such as plotting the evolution of slopes of straight lines fitted to **wellhead** pressure data, as discussed in Appendix C, mitigates these problems to some extent. Regardless of the difficulties in obtaining and interpreting **wellhead** pressure data, it is the easiest and best method of monitoring for leaks in SPR caverns. This is evident from Figures 2 and 3. While a 27.9 bbl/day leak in a 2000 - 4000 ft cavern induces a 90 day change of 3 inches in interface movement, the change in slope of the **wellhead** pressure data is from approximately 0.5 psi/day to 0 psi/day. The change in the slope of the **wellhead** pressure data caused by the crude oil leak is therefore not only more dramatic than the resulting interface movement but **wellhead** pressure data is also much easier to obtain as it is available from surface pressure gauges.

Interface Depth

Cavern Depth

To determine the effect of cavern depth on the relationship between interface movement and leak rate, the changes in interface depths for middle-aged ($t_{\text{start}} = 10$ yrs) cylindrical caverns at three depths, 1500 - 3500 ft, 2000 - 4000 ft, and 2500 - 4500 ft, with 8 different leak rates have been plotted in Figures 7, 8, and 9. From these figures, it is apparent that for a given leak rate, deeper caverns experience greater movements in interface depth than shallow **caverns**. Furthermore, above a certain leak rate, the overall slope of the $\Delta z_i(t)$ data changes from negative to positive, and the leak rate at which this occurs is higher for deeper caverns. For example, for the 2000 - 4000 ft cavern in Figure 8, the interface movement continues its preleak downward trend for leak rates of 1, 5, 10, and 20 bbl/day. For greater leak rates, however, the trend in interface movement is upward after the leak begins at $t = 90$ days. For the deep cavern, 2500 - 4500 ft, shown in Figure 9, the reversal in the direction of interface movement occurs at a higher leak rate. That is, leak rates of 1, 5, 10, 20, 40, and 60 **bbl/day** do not change the preleak downward interface movement, while larger leak rates reverse this trend.

It is also evident from these figures that as the leak rate increases, the drops in interface depth due to brine removal at the 30 day intervals

Repressurization Ratios for 2000-4000 ft Caverns $t_{\text{start}} = 10 \text{ yr}$

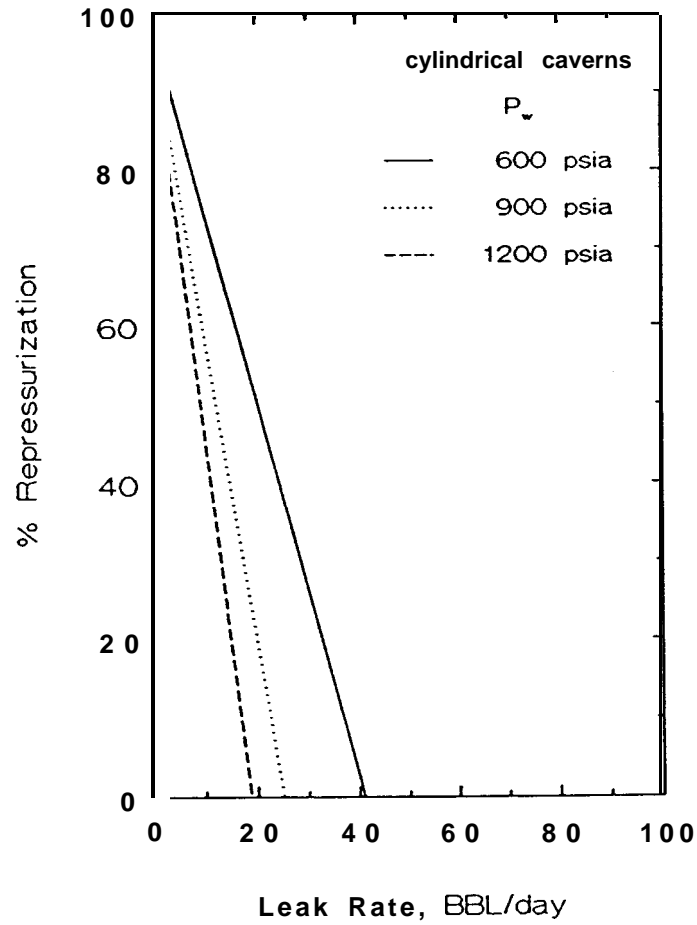


Figure 6. Repressurization ratio vs leak rate for 2000 - 4000 ft cylindrical caverns, 10 years after fill, operated at 600, 900 and 1200 psia.

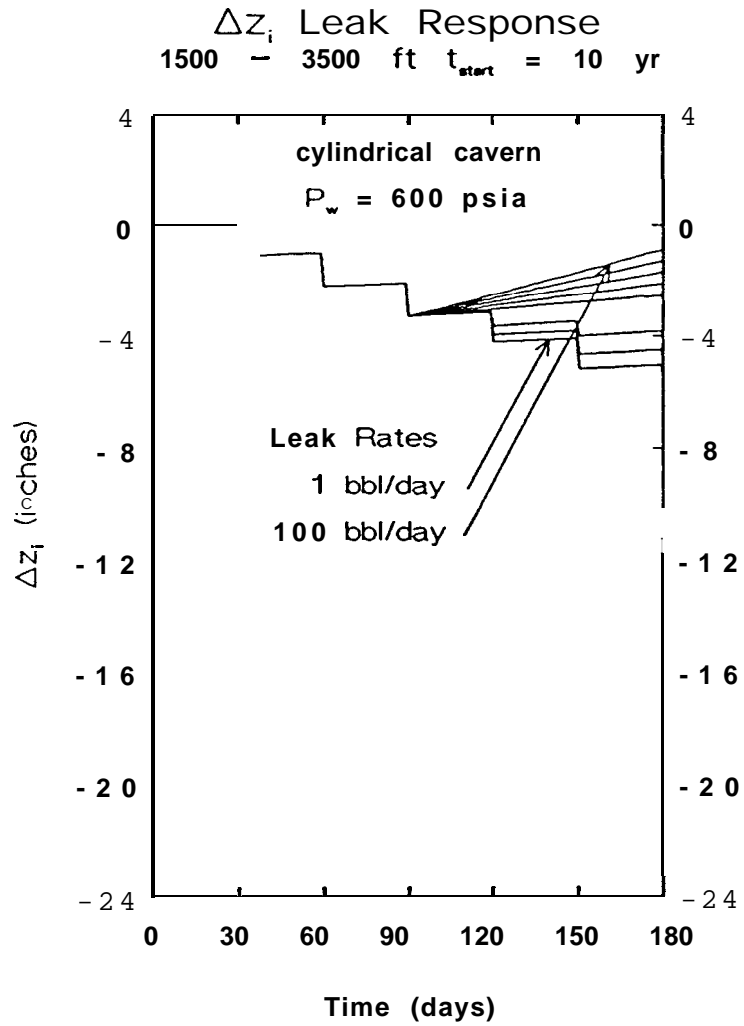


Figure 7. The change in interface depths for a cylindrical cavern, 1500 - 3500 ft, 10 years after fill, operated at 600 psia, with 8 different leak rates (from bottom to top in figure): 1, 5, 10, 20, 40, 60, 80, and 100 bbl/day. All leaks were initiated at $t = 90$ days.

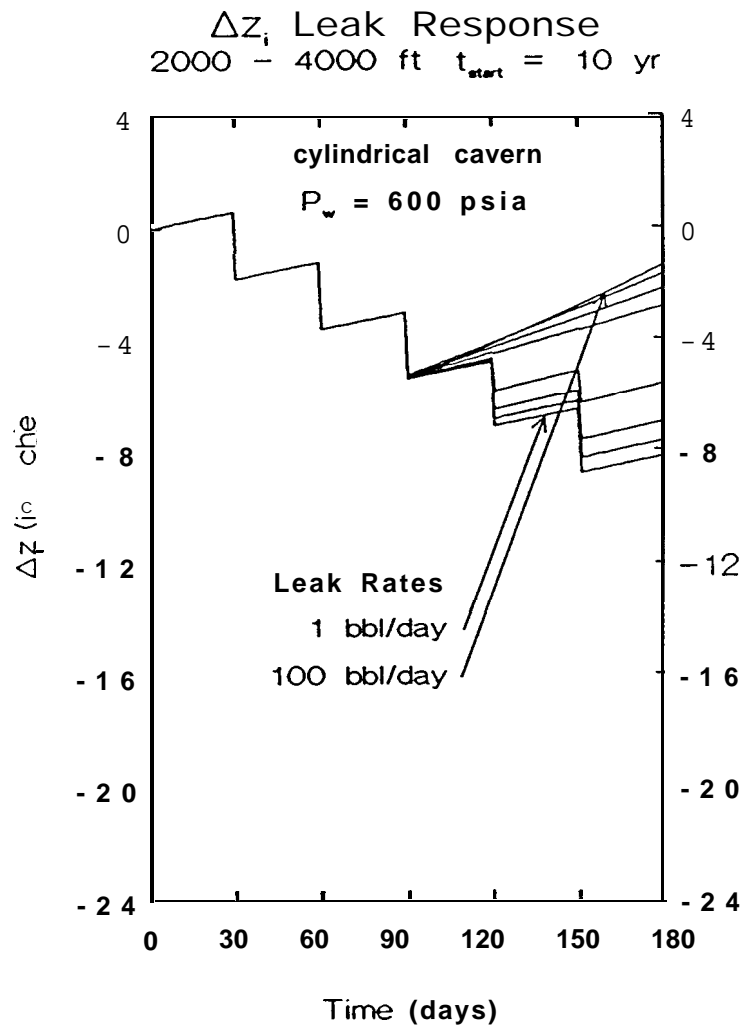


Figure 8. The change in interface depths for a cylindrical cavern, 2000 - 4000 ft, 10 years after fill, operated at 600 psia, with 8 different leak rates (from bottom to top in figure): 1, 5, 10, 20, 40, 60, 80, and 100 bbl/day. All leaks were initiated at $t = 90$ days.

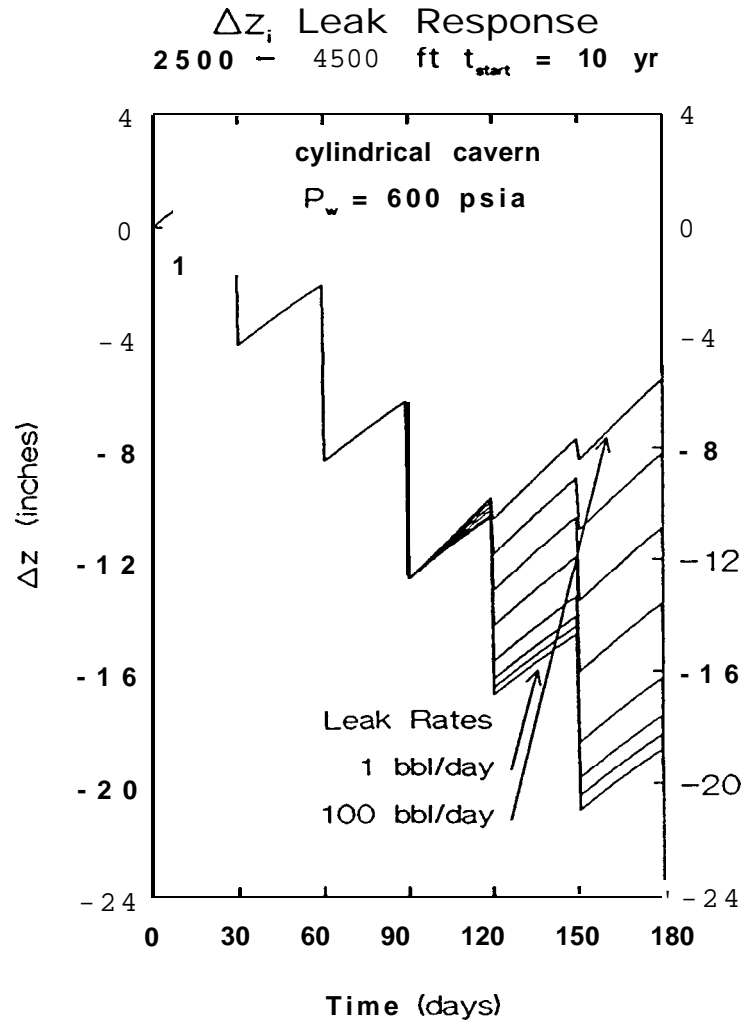


Figure 9. The change in interface depths for a cylindrical cavern, 2500 - 4500 ft, 10 years after fill, operated at 600 psia, with 8 different leak rates (from bottom to top in figure): 1, 5, 10, 20, 40, 60, 80, and 100 bbl/day. All leaks were initiated at $t = 90$ days.

decrease in size and eventually reach zero when the leak rate corresponding to a repressurization ratio of 0% has been reached. For example, for a cylindrical 2000 - 4000 ft cavern operated at a **wellhead** pressure of 600 psia, the leak rate corresponding to a repressurization ratio of 0% is 27.9 **bbl/day** (from Figure 6). Therefore, any leak rate above 27.9 **bbl/day** for this cavern would mean that at the monthly intervals for brine withdrawal, the cavern engineer would find that the cavern had not repressurized to its nominal operating pressure and thus no brine would need to be removed. Thus the plots of interface movement for leak rates above this value should show no signs of brine removal (i.e. no drops in interface depths at 30 day intervals). This can be seen in Figure 8. In this figure, leak rates of 1, 5, 10, and 20 **bbl/day** (all less than the 27.9 **bbl/day** which gives a 0% repressurization ratio) show drops in interface depth at 30 day intervals. The plots of the interface movements for the higher leak rates in this figure are smooth without any signs of periodic brine removal. Thus when the cavern's leak rate exactly balances the volume lost due to cavern creep closure, the cavern repressurizes to its baseline **wellhead** pressure. Note that included in this balance of dynamic cavern behavior is the ongoing thermal equilibration of the cavern and that the more completely equilibrated the cavern is, (i.e. more years since fill), the less thermal equilibration factors into the leak rate/creep closure rate balance which determines the cavern repressurization.

Cavern Shape

Although cavern shape has a small effect on **wellhead** pressure data (Figure 4, it has a large effect on the relationship between interface movement and leak rate. This is evident from Figures 10, 11, and 12, $\Delta z_i(t)$ vs time plots for carrot-shaped caverns at the same depths, leak rates, and cavern ages as in Figures 7, 8, and 9. By comparing the interface movement of caverns identical in depth, **wellhead** pressure, age, and volume, but differing in shape, it is apparent that the interface movement for a given leak rate is more dramatic for carrot-shaped caverns than it is for cylindrical caverns. This is due to the geometric link between cavern shape and volume distribution. That is, for a given volume of fluid loss, the effect on the fluid level (interface depth) will be greater at smaller radii. As can be seen from Figure 1, in the bottom half of the caverns studied in this work, the radius of the carrot-shaped caverns is smaller than that of the cylindrical caverns. Thus, any fluid level movement in the bottom half of these caverns, such as oil/brine interface depth, will be more pronounced for the carrot-shaped caverns than for cylindrical caverns. By comparing the the interface movement figures for cylindrical and carrot-shaped caverns, it is also evident that the difference in interface movement for the two cavern shapes increases with cavern depth. That is, the effect of cavern shape on interface movement at a given leak rate is more pronounced for deeper caverns. This can also be seen from Figure 4, the repressurization ratio/leak rate relationship for cylindrical and carrot-shaped caverns of varying depths.

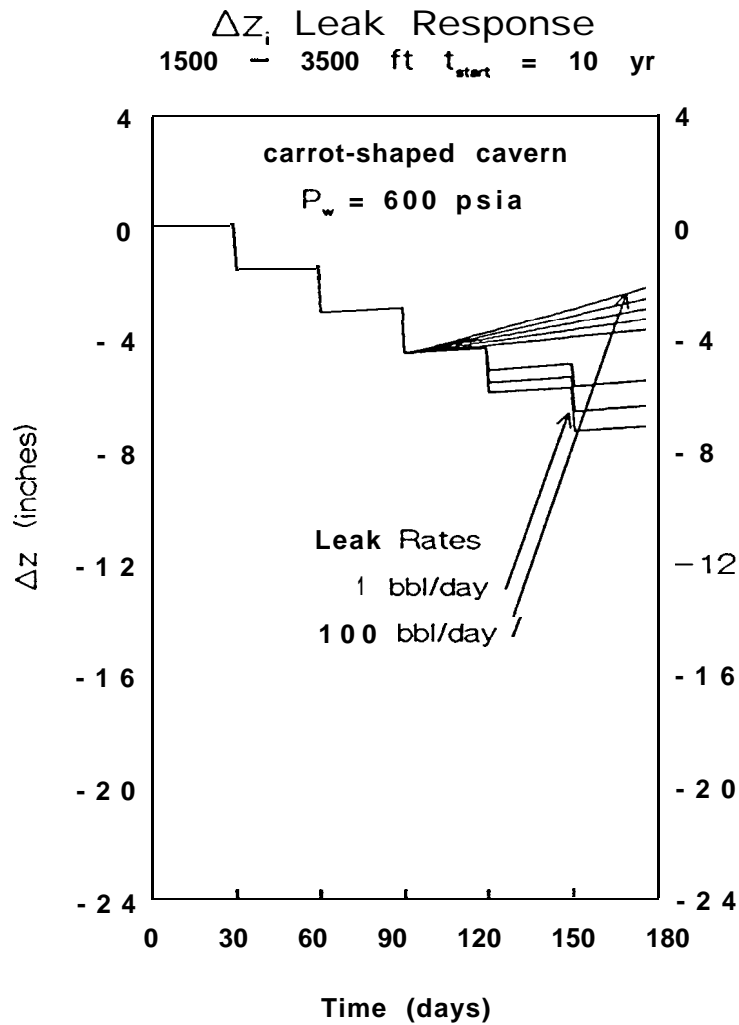


Figure 10. The change in interface depths for a carrot-shaped cavern, 1500 - 3500 ft, 10 years after fill, operated at 600 psia, with 8 different leak rates (from bottom to top in figure): 1, 5, 10, 20, 40, 60, 80, and 100 bbl/day. All leaks were initiated at $t = 90$ days.

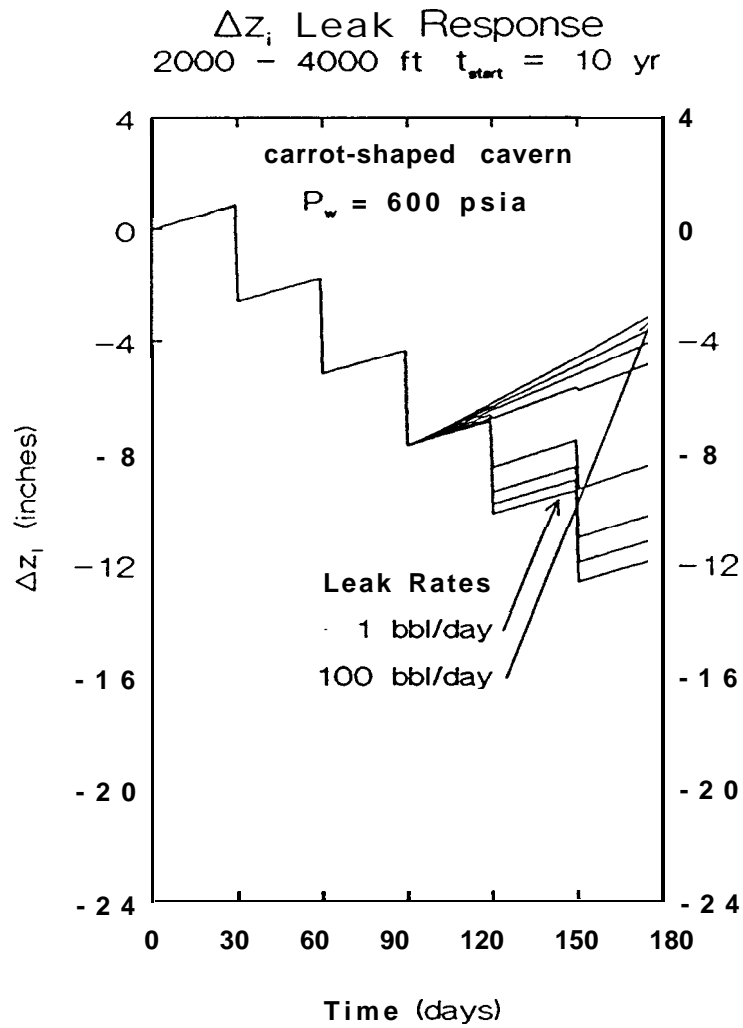


Figure 11. The change in interface depths for a carrot-shaped cavern, 2000 - 4000 ft, 10 years after fill, operated at 600 psia, with 8 different leak rates (from bottom to top in figure): 1, 5, 10, 20, 40, 60, 80, and 100 bbl/day. All leaks were initiated at $t = 90$ days.

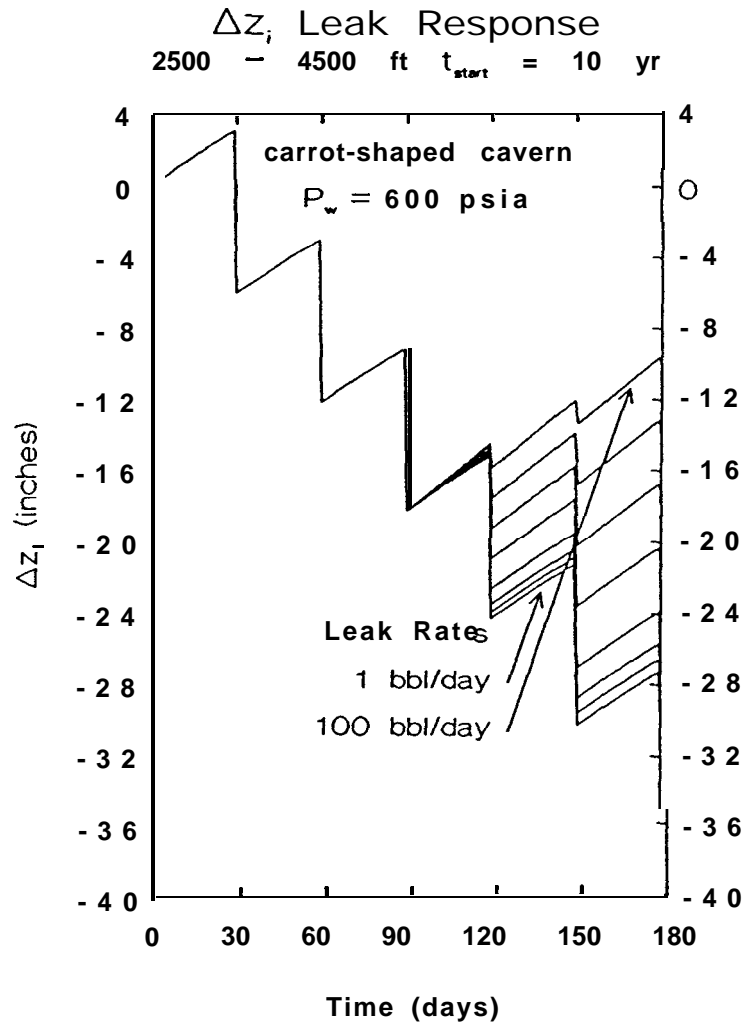


Figure 12. The change in interface depths for a carrot-shaped cavern, 2500 - 4500 ft, 10 years after fill, operated at 600 psia, with 8 different leak rates (from bottom to top in figure): 1, 5, 10, 20, 40, 60, 80, and 100 bbl/day. All leaks were initiated at $t = 90$ days.

Cavern Age

The effect of cavern age on interface movement for varying leak rates can be seen by comparing (Figures 13, 14, 8, and 15) plots of the change in interface movement, $\Delta z_i(t)$, for a 2000 - 4000 ft cylindrical cavern at 4 different ages, 1, 5, 10, and 20 years since fill, respectively. From these figures it is seen that the both the preleak as well as the **postleak** interface movement are more dramatic for younger caverns, a result consistent with Figure 5, a **comparision** of repressurization ratio/leak rate relationships for caverns of varying ages. As stated above, this is due to the fact the the expansion of the cavern fluids due to thermal equilibration is more vigorous for younger caverns (Appendix A). The expansion of the cavern fluids raises the **wellhead** pressure more quickly, thus more brine must be removed to maintain the cavern. The direct result is that a more dramatic drop in interface movement occurs at the 30 day cavern maintenance intervals. Furthermore, the characteristic leak rate which achieves perfectly constant **wellhead** pressure decreases with cavern age. This is easily seen from Figure 5, but also can be detected in Figures 13, 14, 8, and 15 from the number of **postleak** leak rate **curves** which show no drop in interface at the 30 day intervals. The number of these curves increases with cavern age, an indication that older **caverns** experience less repressurization due to lesser changes in fluid temperature.

Cavern Operating Pressure

The relationship between cavern operating pressure and interface movement can be seen in Figures 16 and 17, plots of $\Delta z_i(t)$ vs time for 2000 - 4000 ft cylindrical caverns aged 10 years since fill and operated at 900 and 1200 psia. By comparing Figures 8, 16, and 17, it can be seen that raising the operating pressure and thus reducing the creep rate, results in less dramatic movement of the interface at a given leak rate. In addition, raising the operating pressure from 600 psia to 900 psia has a much greater impact on the interface's response to leak rate than raising the operating pressure from 900 psia to 1200 psia.

The Effects of Thermal Equilibration Decoupled from Cavern Creep Closure

The effect of the thermal equilibration process on the **wellhead** pressure and interface depth can be decoupled from that of cavern creep closure by a simple modification of the model's FORTRAN code which disables the radius change due to creep closure. The modified "no creep" model can then be used to predict the **wellhead** pressure and change in interface depth for a 2000 - 4000 ft cylindrical cavern operated at 600 psia. Next, the difference in **wellhead** pressure and interface depth between the creeping and noncreeping caverns of varying ages can be determined.

Cavern Repressurization

These differences have been plotted in Figures 18 and 19. From Figure 18, it can be seen that the thermal equilibration contribution to the

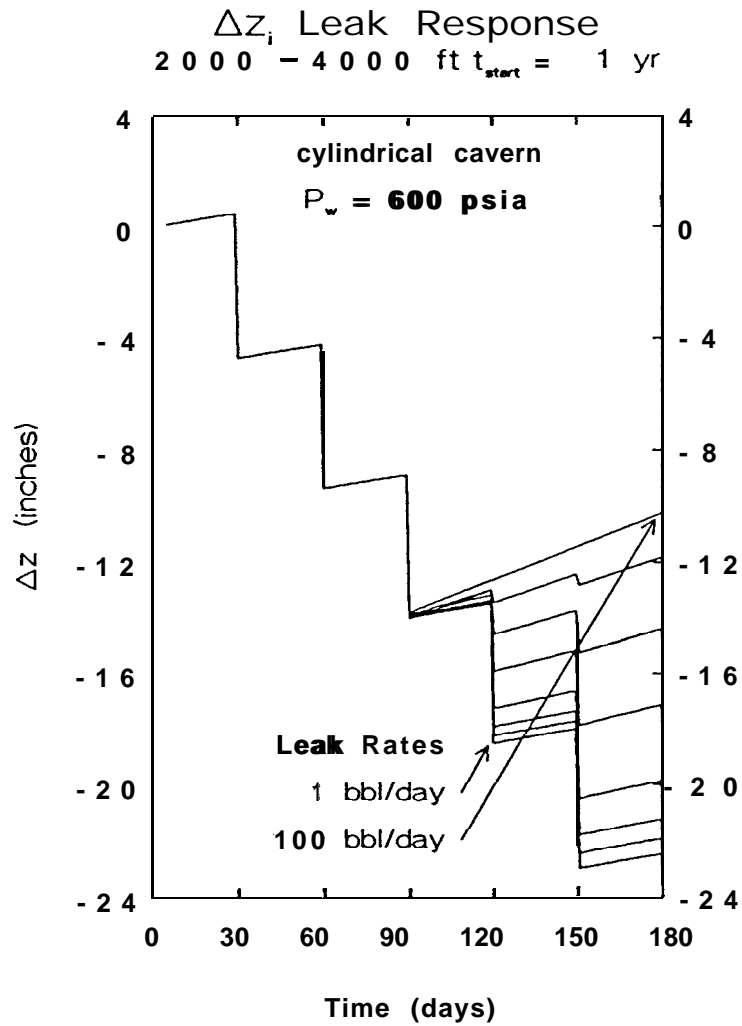


Figure 13. The change in interface depths for a cylindrical cavern, 2000 - 4000 ft, 1 year after fill, operated at 600 psia, with 8 different leak rates (from bottom to top in figure): 1, 5, 10, 20, 40, 60, 80, and 100 bbl/day. All leaks were initiated at $t = 90$ days.

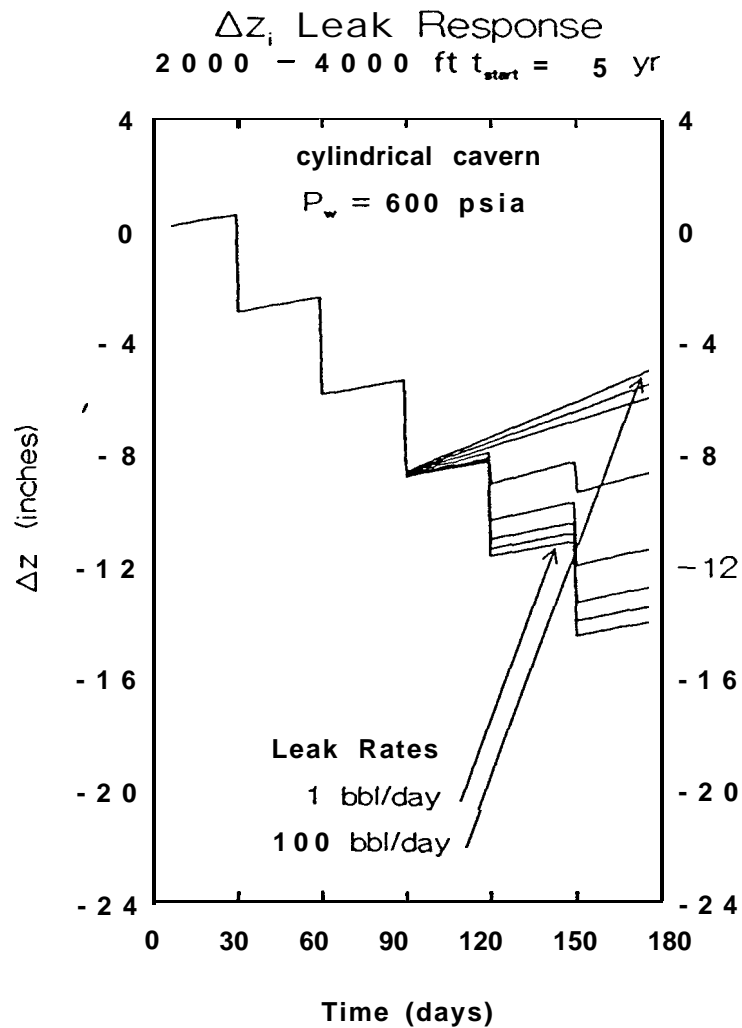


Figure 14. The change in interface depths for a cylindrical cavern, 2000 - 4000 ft, 5 years after fill, operated at 600 psia, with 8 different leak rates (from bottom to top in figure): 1, 5, 10, 20, 40, 60, 80, and 100 bbl/day. All leaks were initiated at $t = 90$ days.

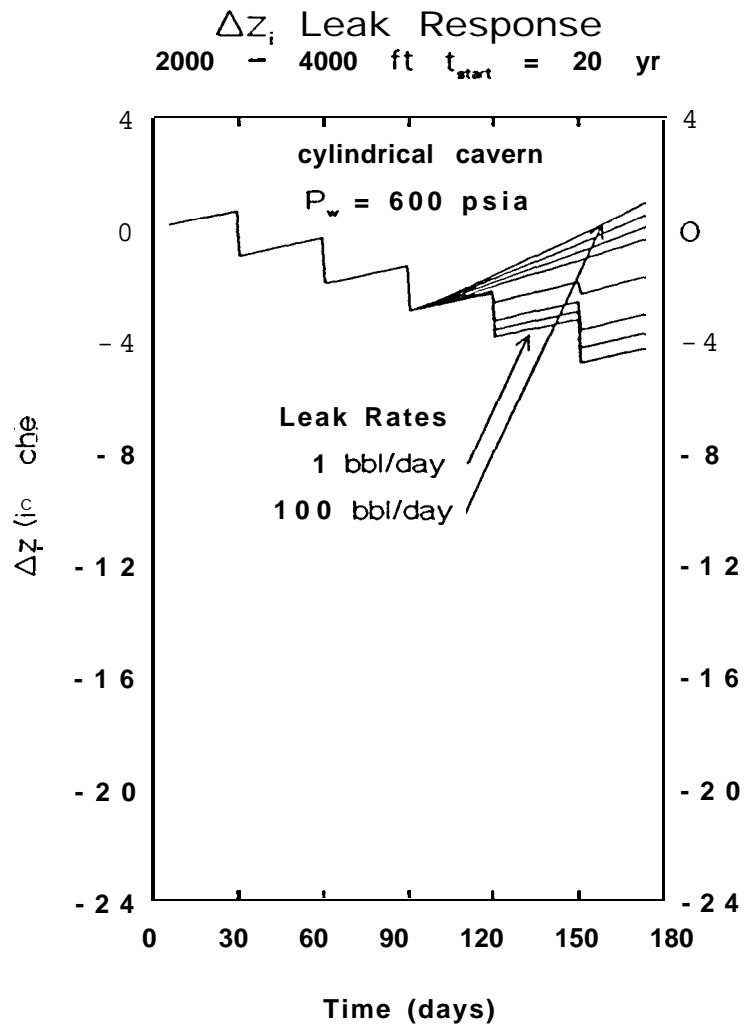


Figure 15. The change in interface depths for a cylindrical cavern, 2000 - 4000 ft, 20 years after fill, operated at 600 psia, with 8 different leak rates (from bottom to top in figure): 1, 5, 10, 20, 40, 60, 80, and 100 bbl/day. All leaks were initiated at $t = 90$ days.

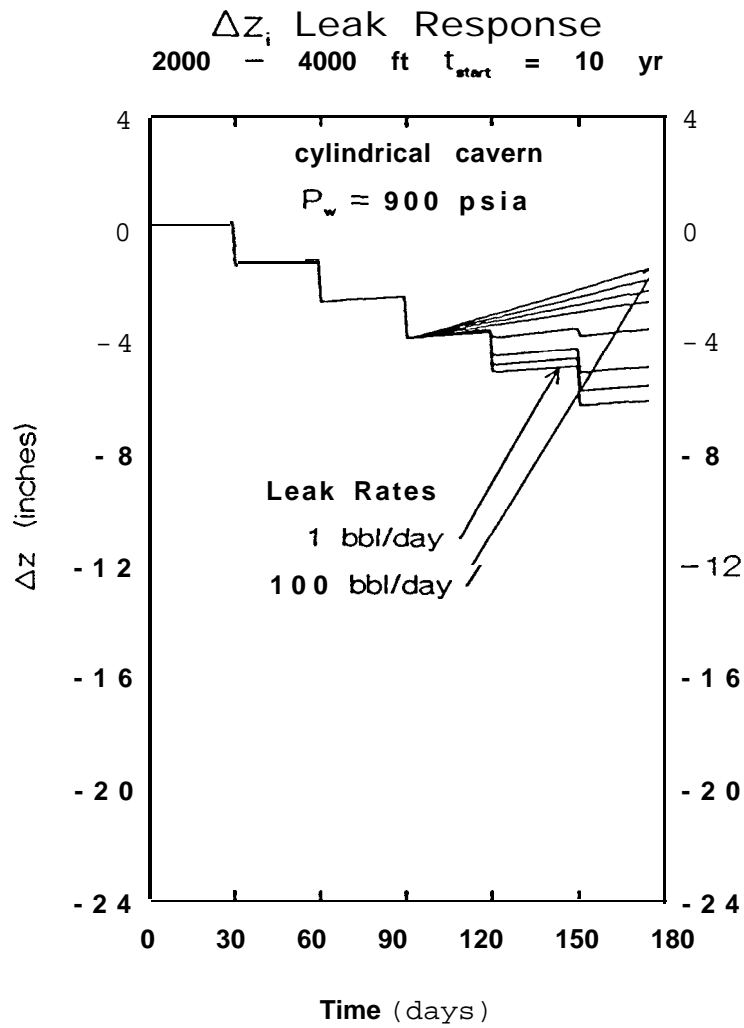


Figure 16. The change in interface depths for a cylindrical cavern, 2000 - 4000 ft, 10 years after fill, operated at 900 psia, with 8 different leak rates (from bottom to top in figure): 1, 5, 10, 20, 40, 60, 80, and 100 bbl/day. All leaks were initiated at $t = 90$ days.

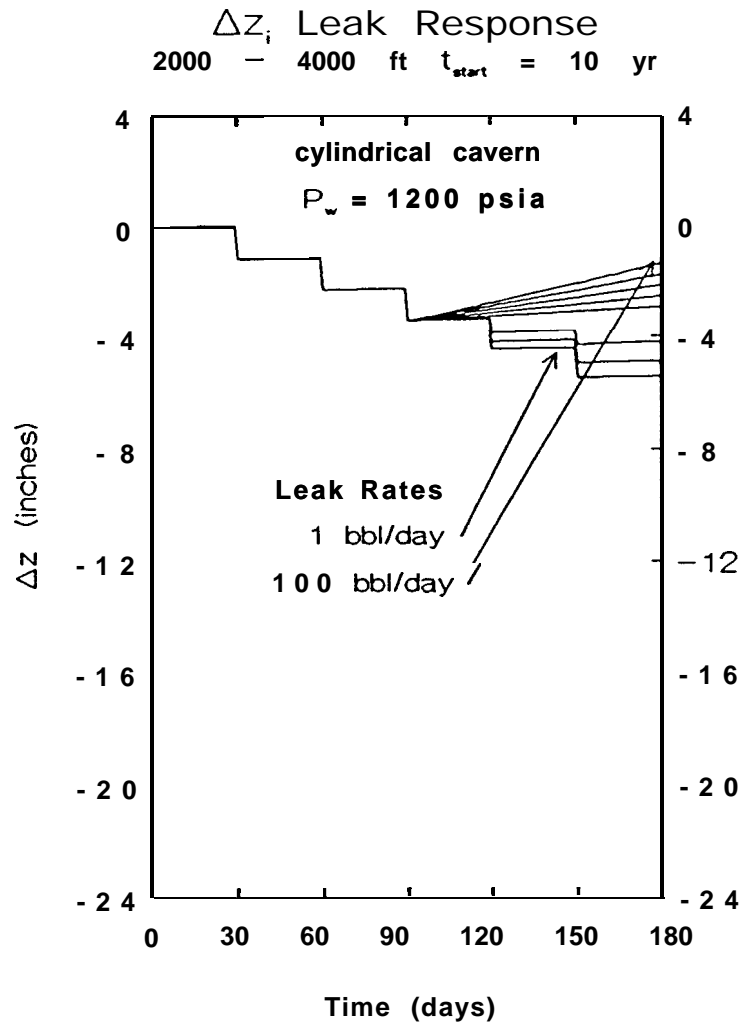


Figure 17. The change in interface depths for a cylindrical cavern, 2000 - 4000 ft, 10 years after fill, operated at 1200 psia, with 8 different leak rates (from bottom to top in figure): 1, 5, 10, 20, 40, 60, 80, and 100 bbl/day. All leaks were initiated at $t = 90$ days.

Difference in Cavern Repressurization Between Creeping and Noncreeping Caverns

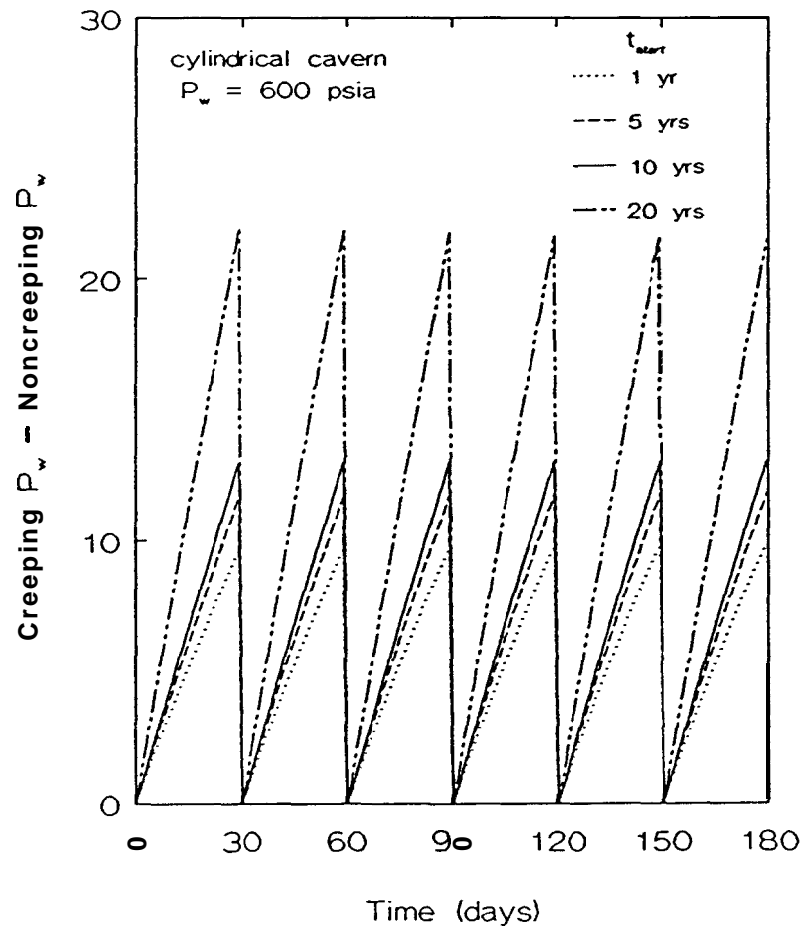


Figure 18. The difference in cavern repressurization between creeping and noncreeping caverns aged 1, 5, 10, and 20 years since fill.

Difference in interface Depth Between Creeping and Noncreeping Caverns

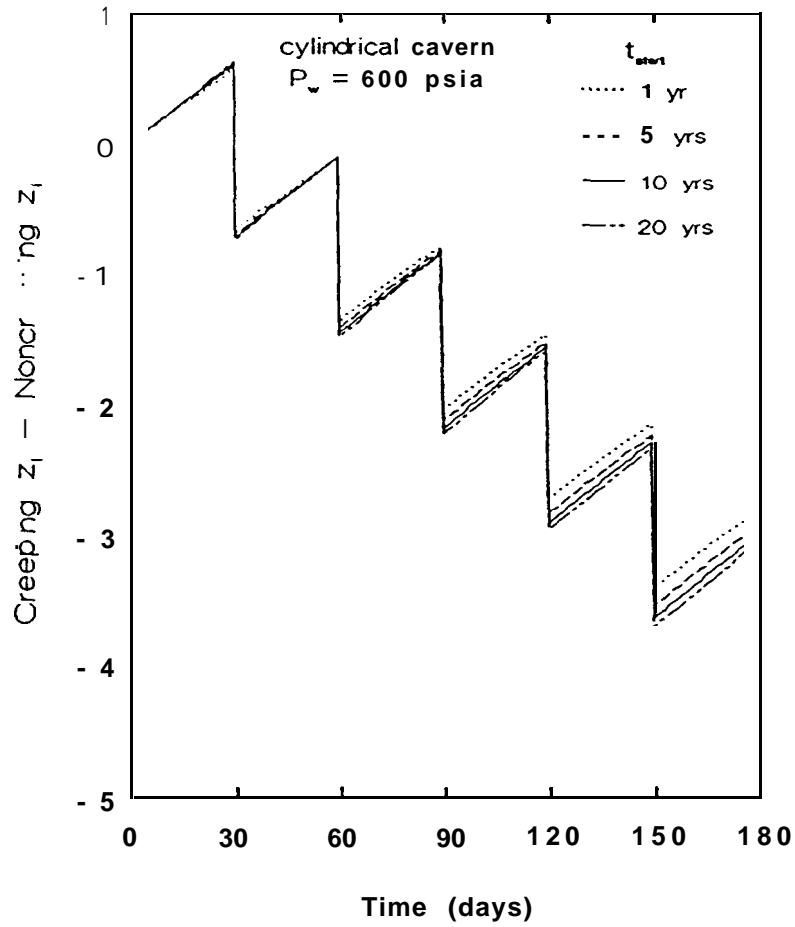


Figure 19. The difference in interface depth between creeping and noncreeping caverns aged 1, 5, 10, and 20 years since fill.

cavern repressurization is decreases with increasing age. That is, the difference between the creeping and noncreeping cavern **wellhead** pressures is the smallest for the youngest cavern, $t_{\text{start}} = 10$ years, and increases with cavern age. Note that this difference is 0 at the 30 day intervals where brine is automatically removed in order to regain the cavern operating pressure, 600 psia, in both cases.

Interface Depth

Figure 19 is a plot of the differences in interface depth between the creeping and noncreeping cavern. As the z ordinate of the model is taken to positively increase with depth, negative values of this difference parameter indicate that the noncreeping interface depth is deeper (mathematically more positive) than the creeping interface depth. This is due to creep closure which moves the interface upward. Furthermore, note that the results for this difference for caverns of different ages spread out with time. Cavern age influences the rate of cavern repressurization, and thus the volume of brine needed to be removed to bring the **wellhead** pressure back to its operational value, V_{BR} (volume of brine removed). The volume of brine removed at these 30 day intervals directly affects the interface depth and this effect is cumulative, that is, with each brine removal, the difference in interface depth between the creeping and noncreeping caverns grows by an amount representative of the difference in V_{BR} for creeping and noncreeping caverns.

Summary

The viability of using interface movement measurements to detect leaks in SPR caverns is perhaps best investigated by comparing the interface movement of a leaking cavern to that of a nonleaking cavern for a variety of cavern configurations. This is easily done with the above data, and has been summarized in Table 1. The far right-hand column in this table, $z_i(180 \text{ days}, 100 \text{ bbl/day}) - z_i(180 \text{ days}, 0 \text{ bbl/day})$ is simply the difference in final interface depth (at 180 days) for identical caverns which experience 100 **bbl/day** and 0 **bbl/day** leaks. This parameter reflects how the interface movement, $z_i(t)$, would change due to a 100 **bbl/day** leak, and must exceed the estimated error inherent in interface movements.

Table 1

Cavern Depth	Wellhead Pressure (psia)	t_{start} (yr)	Cavern Shape	z_i (180 days, 100 bbl/day) z_i (180 days, 0 bbl/day)
1500-3500 ft	600	10	cylindrical	5.4
2000-4000 ft	600	10	cylindrical	- 9.4
2500-4500 ft	600	10	cylindrical	- 18.7
1500-3500 ft	600	10	carrot-shaped	- 6.9
2000-4000 ft	600	10	carrot-shaped	- 12.5
2500-4500 ft	600	10	carrot-shaped	- 25.4
2000-4000 ft	600	1	cylindrical	- 17.4
2000-4000 ft	600	5	cylindrical	- 12.6
2000-4000 ft	600	20	cylindrical	- 7.2
2000-4000 ft	900	10	cylindrical	- 6.5
2000-4000 ft	1200	10	cylindrical	- 5.3

CONCLUSIONS

The movement of the oil/brine interface in SPR caverns is dependent on the relative rates of cavern creep, brine removal, crude oil leakage, and cavern pressurization due to the thermal equilibration process. These relationships are further influenced by cavern depth, **wellhead** pressure, and cavern shape. The largest interface movements are found in caverns with high creep rates, such as deep caverns or those operated at lower pressures, and young caverns, due to the large repressurization rates these caverns experience as a result of thermal equilibration of the oil/salt system. Carrot-shaped caverns experience greater interface movement than right-cylindrical caverns for a given leak rate.

As seen from Table 1, the interface depth response to large leaks, 100 bbl/day, ranges from 5 to 25 inches over a 3 month leak period. While interface depth can be measured to within a couple inches, for these measurements to be utilized in detecting leaks, the other cavern phenomena which contribute to interface movement must be adequately quantified. In particular, the cavern thermal equilibrium process has a large impact on interface movement in young caverns. In addition, ~~leaks~~ ~~smaller than 100 bbl/day may be lost in the error inherent in interface~~ ~~depth~~ measurements. Thus it must be concluded that **wellhead** pressure data is the most reliable method of detecting SPR leaks. However, in cases of small leaks, scattered **wellhead** pressure data, or when a cavern as had several interruptions, interface depth measurements provide additional insight to cavern behavior.

REFERENCES

Biringer, K. L., 'Strategic Petroleum Reserve (SPR) Long-Term Monitoring System Pressure Data Analysis,' Sandia Laboratories Report SAND87-0706 (1987).

Heffelfinger, G. S., 'Creep Closure of Salt Caverns in the Strategic Petroleum Reserve', Sandia Laboratories Report SAND 90-2614 (1991).

Roark, R. J., Formulas for Stress and Strain, 3rd Edition, McGraw-Hill, New York (1954).

Tomasko, D., 'Preliminary SPR Thermal Model Description and Results for WH-11 and BM-4', Sandia Laboratories Report SAND84-1957 (1985).

Wynn, K. D., 'Cavern Pressure Monitoring and Operational Control Procedure,' U.S. Department of Energy Strategic Petroleum Reserve Publication **D506-01724-09** (1990).

Appendix A

Temperature Models

Tomasko has **modelled** the temperature evolution of an SPR cavern filled with crude oil at 294.4 K (70°F) (Tomasko, 1985) and compared the results to real SPR caverns. An adequate representation of this temperature evolution is

$$T_{oil}(t) = T_f + (1 - e^{-t/\tau})(T_{ms} - T_f) \quad (A-1)$$

where $T_{oil}(t)$ is the time evolution of the crude oil, T_f the fill temperature, T_{ms} the mean temperature of the salt (taken as the **salt** temperature at the cavern midpoint), τ the time constant of the thermal equilibration, and t time. Throughout this work, τ was taken to be 2500 days as suggested by Tomasko. The salt temperature profile from which T_{ms} is taken has been discussed previously (Heffelfinger, 1991) and yields values of 318.9 K (114°F), 322.8 K (121°F), and 326.7 K (128°F) for caverns 1500 - 3500 ft, 2000 - 4000 ft, and 2500 - 4500 ft deep, respectively.

Using this model of the temperature of the oil, the time evolution for SPR crude oil can be plotted as a function of time for the three cavern depths investigated in this work. This has been done in Figure A-1 where it can be seen that, for all three depths, the oil starts at the fill temperature, 294.4 K (70°F), and **reaches** the mean salt temperature, T_{ms} , after approximately 30 years. Throughout this work, four different cavern ages (defined as time since fill) have been investigated, $t_{start} = 1, 5, 10$, and 20 years. The effect of the oil's temperature evolution on the interface movement will be most profound in regimes where the temperature changes quickly with time. From Figure A-1, it is easily seen that this occurs at small values of time. This figure can be expanded for the depths and cavern ages investigated in this work as in Figures A-2, A-3, and A-4, temperature evolution plots for caverns 1500 - 3500 ft, 2000 - 4000 ft, and 2500 - 4500 ft deep, respectively. From these figures the relative changes in slope of the temperature evolution can be seen for the different time regimes investigated.

Finally, a 2000 - 4000 ft cylindrical cavern, operated at 600 psia, which experiences 1 and 100 **bbl/day** leaks has been **modelled** using three different oil temperature models. The first model employs a constant (with time as well as depth) oil temperature equal to the mean salt temperature. The second model is also constant with **time** but varies with depth and is equal to the salt temperature profile. This is the model previously employed by this simplified creep model for studies not strongly affected by the oil temperature profile (Heffelfinger, 1991). The third model is the time evolution discussed above, equation A-1, for four different cavern ages: $t_{start} = 1, 5, 10$, and 20 years.

Temperature Evolution Model

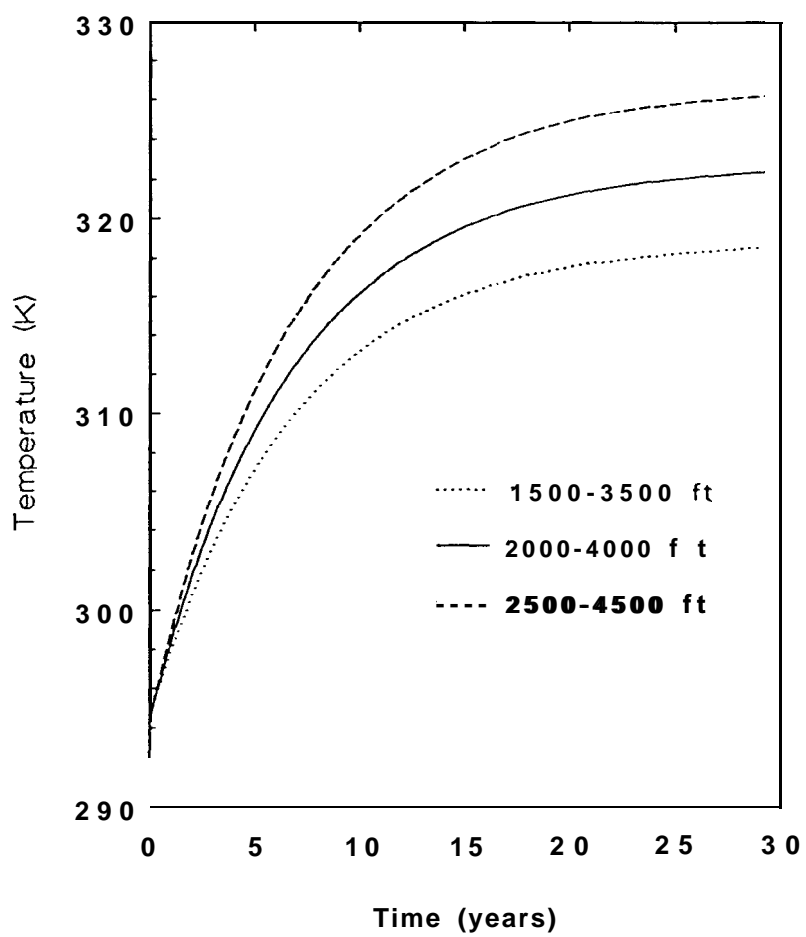


Figure A-1. The temperature evolution, $T(t)$, for 1500 - 3500, 2000 - 4000, and 2500 - 4500 ft caverns after the work of Tomasko (Tomasko, 1985).

Expanded Temperature Evolution Model

1500 - 3500 ft

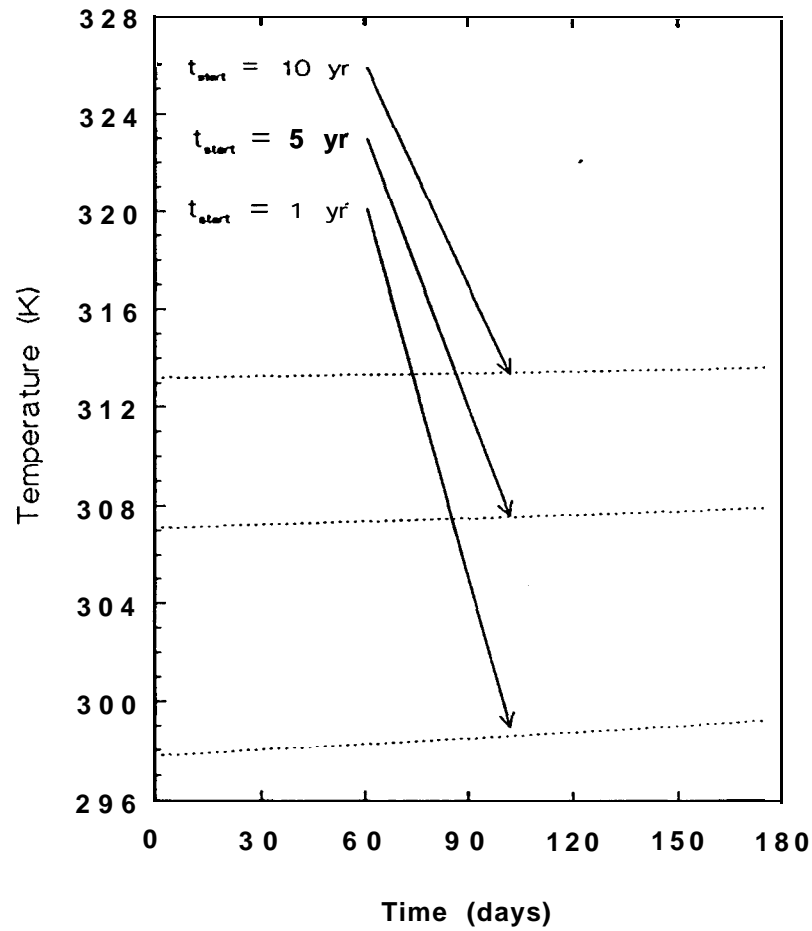


Figure A-2. An expansion of the $t_{\text{start}} = 1, 5, 10$, and 20 year time regimes of the $T(t)$ profile (Figure A-1) for a 1500 - 3500 ft deep cavern ($t_{\text{start}} =$ time since fill).

Expanded Temperature Evolution Model 2000 - 4000 ft

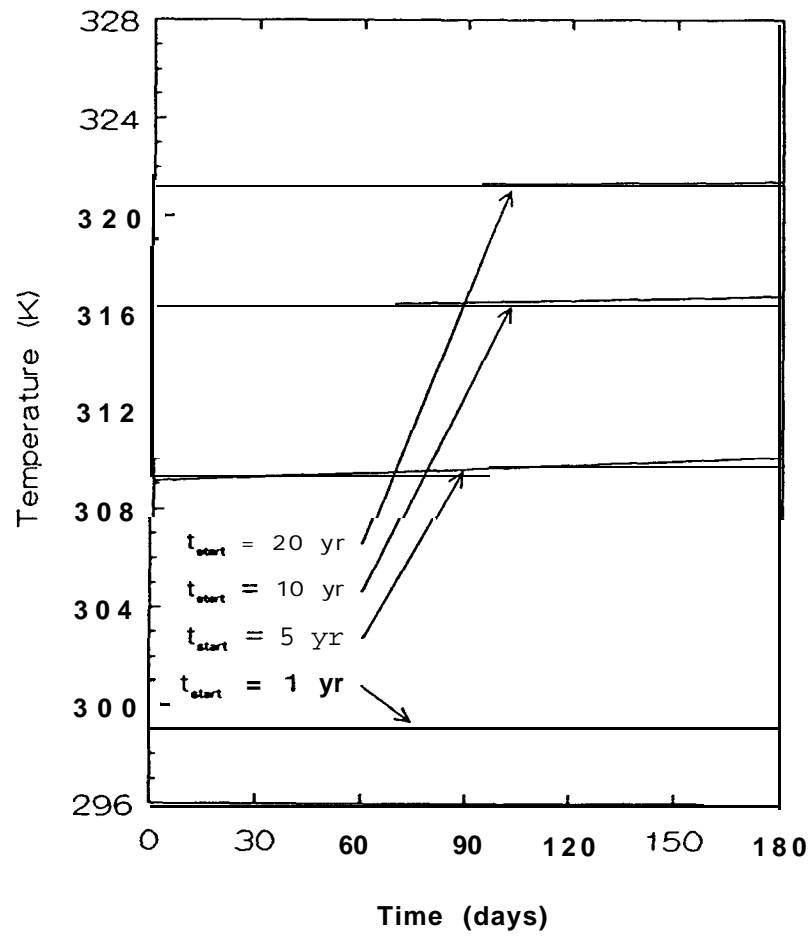


Figure A-3. An expansion of the $t_{start} = 1, 5, 10,$ and 20 year time regimes of the $T(t)$ profile (Figure A-1) for a $2000 - 4000$ ft deep cavern ($t_{start} =$ time since fill).

Expanded Temperature Evolution Model 2500 - 4500 ft

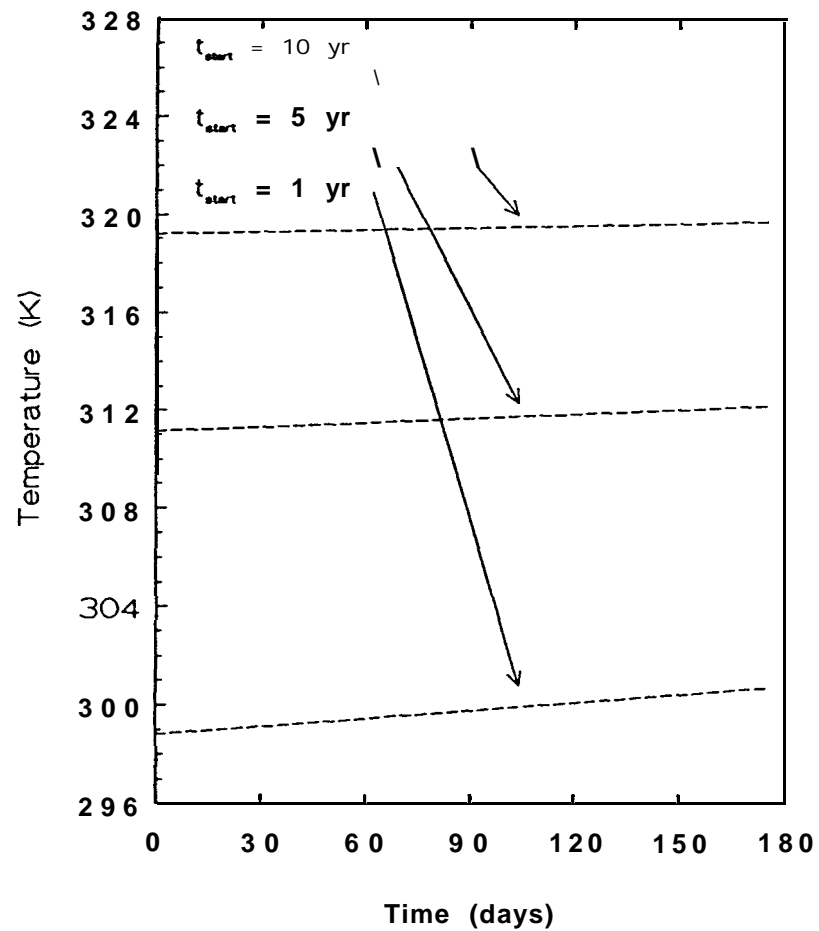


Figure A-4. An expansion of the $t_{\text{start}} = 1, 5, 10$, and 20 year time regimes of the $T(t)$ profile (Figure A-1) for a 2500 - 4500 ft deep cavern ($t_{\text{start}} =$ time since fill).

As done throughout this work, the leak was initialized after three months of creep closure and allowed to continue for three additional months. For this period, the differences between the models for total volume lost to creep closure, interface depth, and **wellhead** pressure, determined as a percent difference were negligible. However, the change in interface movement, or first derivative of $z(t)$, the evolution of the interface depth with time, is much more sensitive to changes in the oil temperature model. This can be seen from Figures A-5 and A-6, the results for interface movement for this cavern with the different temperature models. It can be seen from these figures that modelling the temperature as time invariant, whether invariant with depth or equal to the salt temperature profile, produces much the same results for change in interface movement. The time dependent oil temperature, however, deviated from these results. Furthermore, this difference increased with decreasing cavern age. Thus, the temperature model employed to study interface movement significantly affects the results, particularly for young caverns, i.e. those within one year of fill.

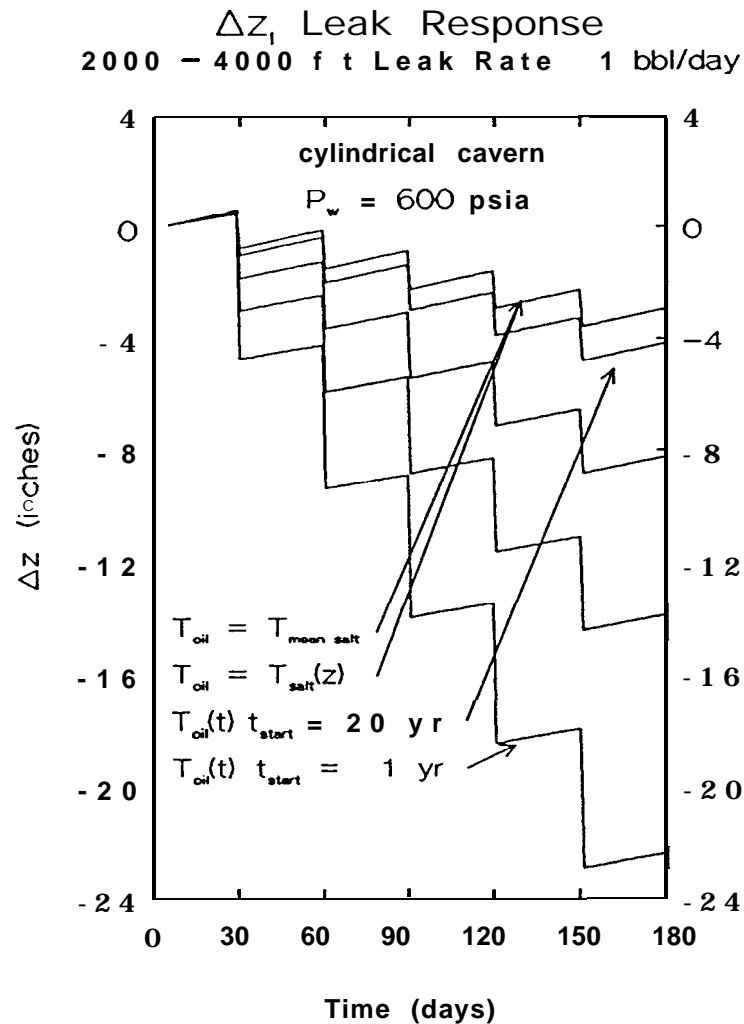


Figure A-5. The change in interface depths for a cylindrical cavern, 2000 - 4000 ft deep, experiencing a 1 bbl/day, with 3 different oil temperature models. $T_{oil} = T_{mean\ salt}$ indicates a time and depth invariant oil temperature profile which is equal to the mean temperature of the surrounding salt. $T_{oil} = T_{salt}(z)$ represents a time-invariant oil profile equal to that of the surrounding salt. $T_{oil}(t)$ represents a time variant and depth invariant oil temperature according to equation A-1. Four different values of t_{start} are shown: 1, 5, 10, and 20 years (since fill). Note that the results for $T_{oil} = T_{mean\ salt}$ are identical to those for $T_{oil} = T_{salt}(z)$.

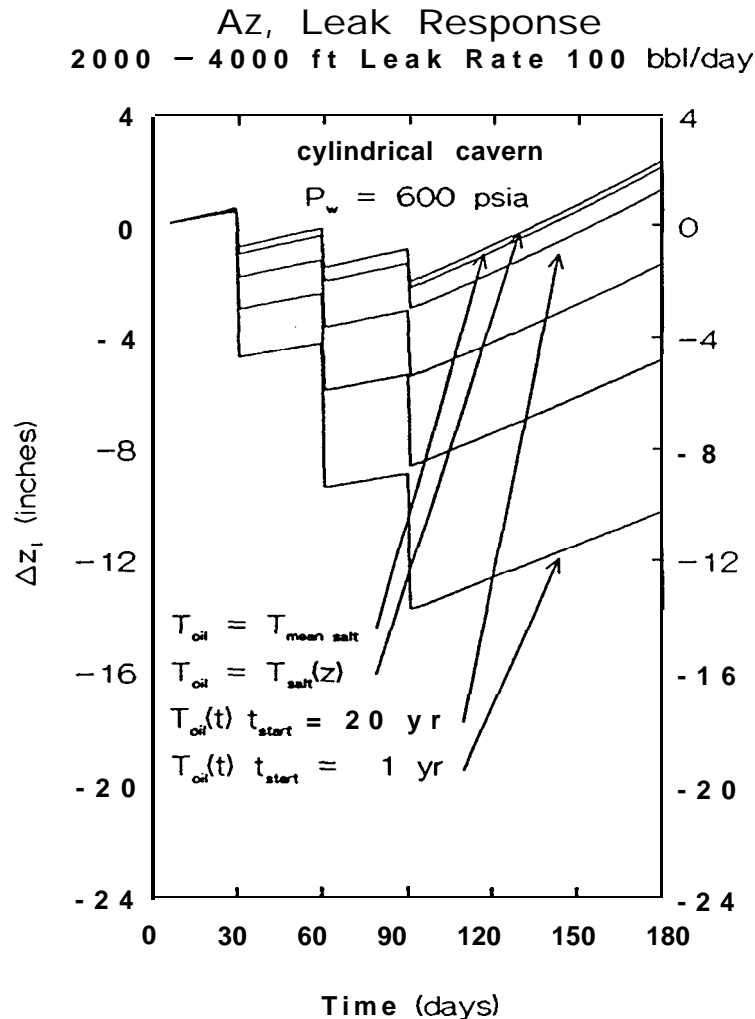


Figure A-6. The change in interface depths for a cylindrical cavern, 2000 - 4000 ft deep, experiencing a 100 bbl/day, with 3 different oil temperature models. $T_{oil} = T_{mean\ salt}$ indicates a time and depth invariant oil temperature profile which is equal to the mean temperature of the surrounding salt. $T_{oil} = T_{salt}(z)$ represents a time-invariant oil profile equal to that of the surrounding salt. $T_{oil}(t)$ represents a time variant and depth invariant oil temperature according to equation A-1. Four different values of t_{start} are shown: 1, 5, 10, and 20 years (since fill).

Appendix B

The Elastic Response of the Cavern

The elastic (time-independent) response of the cavern is relevant only in situations where the cavern pressure changes. This can be seen from the equation governing the elastic response for cylindrical geometry (Roark 1954):

$$\Delta r = - \left(\frac{\Delta p \cdot r}{E_m} \right) (1 - \nu) \quad (B-1)$$

In this equation, Δr is the change in radius, Δp the change in pressure, r the radius, E_m the modulus of elasticity, and ν is Poisson's ratio.

Removing any cavern fluids results in changes in cavern pressure, therefore, the cavern's elastic response may well contribute appreciably to cavern parameters such as repressurization rate and interface movement. Thus the model previously discussed (Heffelfinger, 1991) was modified to include the cavern's elastic response for this work.

Appendix C

Two Methods of Cavern Maintenance

SPR caverns are continuously pressurizing, therefore they require regular maintenance. In particular, to preserve cavern integrity, the cavern pressure at the casing seat must not exceed the lithostatic pressure at the depth of the casing seat. If this does occur, the salt surrounding the casing seat will be forced outward, enabling a hydrodynamic pressure transfer of the cavern pressure up the outside of the casing to the salt surrounding the casing. This in turn, increases the outward salt movement, eventually resulting in cavern failure as the casing-salt seal is no longer able to contain cavern pressure.

Cavern pressurization due to creep closure is controlled by the cavern engineer by removing brine from the cavern. Given the fact that the evolution of the **wellhead** pressure, $P_w(t)$, provides the best means of monitoring SPR caverns for fluid loss, the brine removal process must be carried out in a way that best preserves the value of the **wellhead** pressure data for leak detection. This may be accomplished by two different methods.

In the first method, brine is removed from the cavern at regular time intervals. The resulting **wellhead** pressure data will appear as the solid line in Figure C-1. In this figure, the cavern has pressurized from its baseline pressure of 600 psia to a maximum of approximately 616 psia in 30 days. At this point, and at 30 day intervals thereafter, the cavern was bled to 600 psia. At 90 days, this cavern experienced a 5 bbl/day leak. From Figure C-1, it can be seen that the effect of this leak on the **wellhead** pressure data was that the pressure of the cavern at the end of the 30 day brine removal intervals was less than that previously, down to approximately 614 psia from 616 psia. Thus, if the cavern were operated in this manner, to detect the leak the cavern engineer would need to notice that the cavern was not pressurizing to as high a pressure as previously for the same time period, 30 days.

The second method, brine removal when the cavern reaches some maximum pressure, is the method used by the SPR (Wynn 1990). In this method, brine is removed from the cavern once the cavern pressure reaches a predetermined maximum. For the cavern in Figure C-1, this pressure would have been 614 psia. Prior to the leak at 90 days, the cavern engineer would have removed brine once the cavern reached 616 psia, which in this case corresponded 30 day intervals. However, after the leak, the cavern pressure would take longer to reach 616 psia, as shown by the dotted line in Figure C-1. Thus to detect the leak, the cavern engineer would need to notice that the cavern was taking longer to repressurize. In Figure C-2, similar results for the same cavern with a 10 bbl/day leak, have been plotted. The differences between the two methods of cavern operation are similar to those in Figure C-1, but more exaggerated.

If the slope of the $P_w(t)$ line is plotted as a function of time, the resulting graph is independent of the method used for cavern maintenance.

Wellhead Pressure Leak Response 2000 - 4000 ft 5 bbl/day

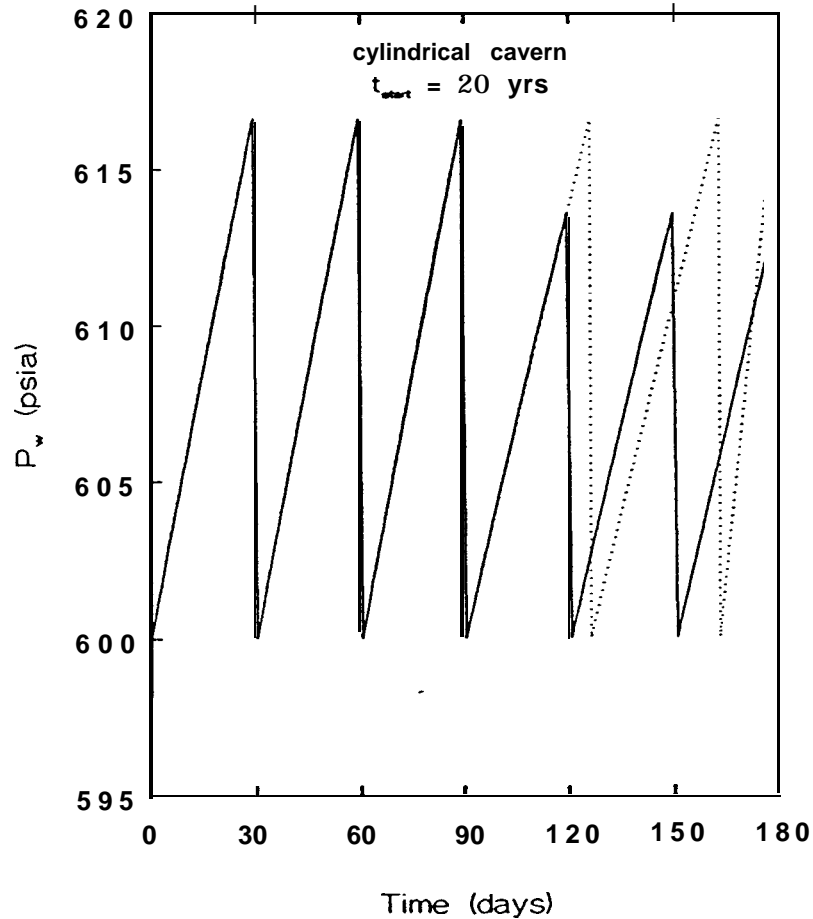


Figure C-1. **Wellhead** pressure evolution, $P_{w,,}(t)$, for a 2000 - 4000 ft cavern, 20 years after fill, which experiences a 5 bbl/day leak at 90 days. The preleak ($t < 90$ days) solid line represents the **wellhead** pressure evolution whether the cavern is operated with brine removal at regular intervals or with brine removal upon reaching some maximum value of **wellhead** pressure. The **postleak** ($t > 90$ days) indicates the **wellhead** pressure evolution if the cavern is operated with brine removal at regular intervals. The **postleak** ($t > 90$ days) dotted line represents the **wellhead** pressure evolution if the cavern is operated with brine removal when the **wellhead** pressure reaches **some maximum** value.

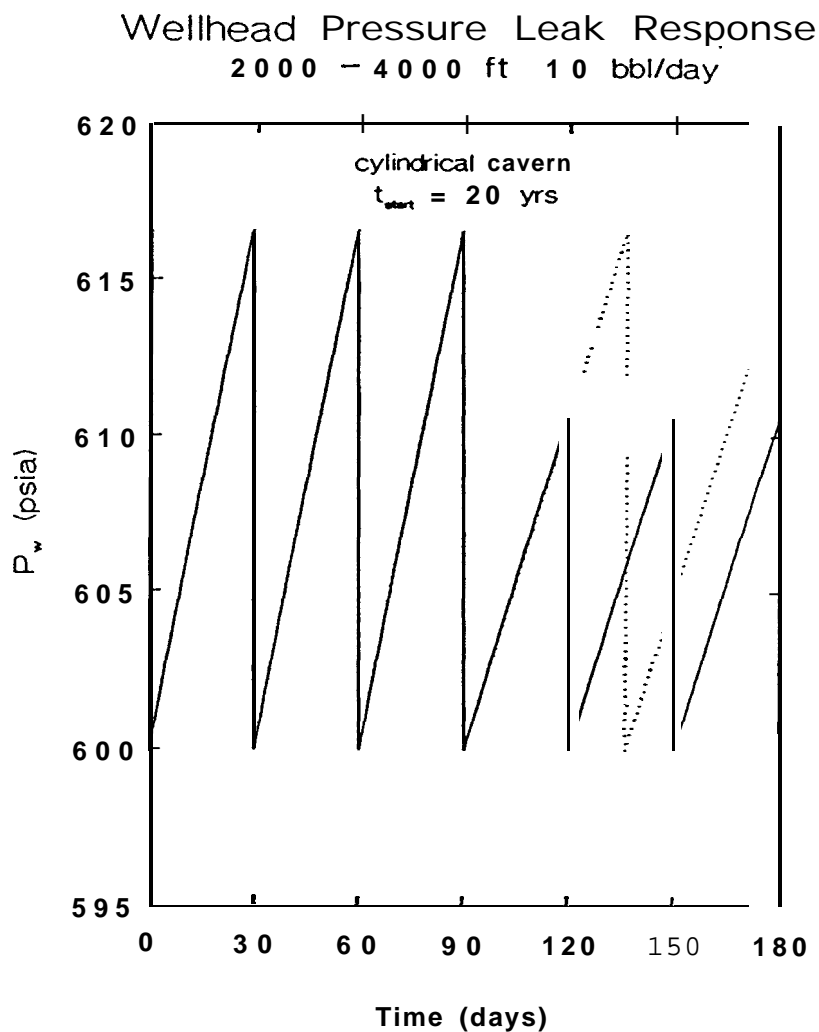


Figure C-2. **Wellhead** pressure evolution, $P_w(t)$, for a 2000 - 4000 ft cavern, 20 years after fill, which experiences a 10 bbl/day leak at 90 days. The preleak ($t < 90$ days) solid line represents the **wellhead** pressure evolution whether the cavern is operated with brine removal at regular intervals or with brine removal upon reaching some maximum value of **wellhead** pressure. The **postleak** ($t > 90$ days) indicates the **wellhead** pressure evolution if the cavern is operated with brine removal at regular intervals. The **postleak** ($t > 90$ days) dotted line represents the **wellhead** pressure evolution if the cavern is operated with brine removal when the **wellhead** pressure reaches some maximum value.

This has been done for the above cavern, for leaks beginning at $t = 90$ **days**, with rates of 1, 5, 10, and 20 bbl/day. This is generally the type of information the cavern engineer would use when examining $P,(t)$ data for evidence of leaks. The repressurization rate, psi/day, is simply the slope of the $P,(t)$ data and is unique for caverns which have been filled with oil long enough such that the cavern has stabilized with respect to **postleak** creep closure, approximately 2 years for typical SPR caverns. After this time, this ratio will change slightly at the cavern thermally equilibrates. Because the $P,(t)$ data is generally scattered, the cavern engineer curve fits straight lines to sections of data and compares the slopes of these lines. A leak will appear as a decrease in the repressurization rate, as seen for the 4 leak rates: 1, 5, 10, and 20 bbl/day, shown in Figure C-3.

Wellhead Pressure Leak Response 2000 - 4000 ft

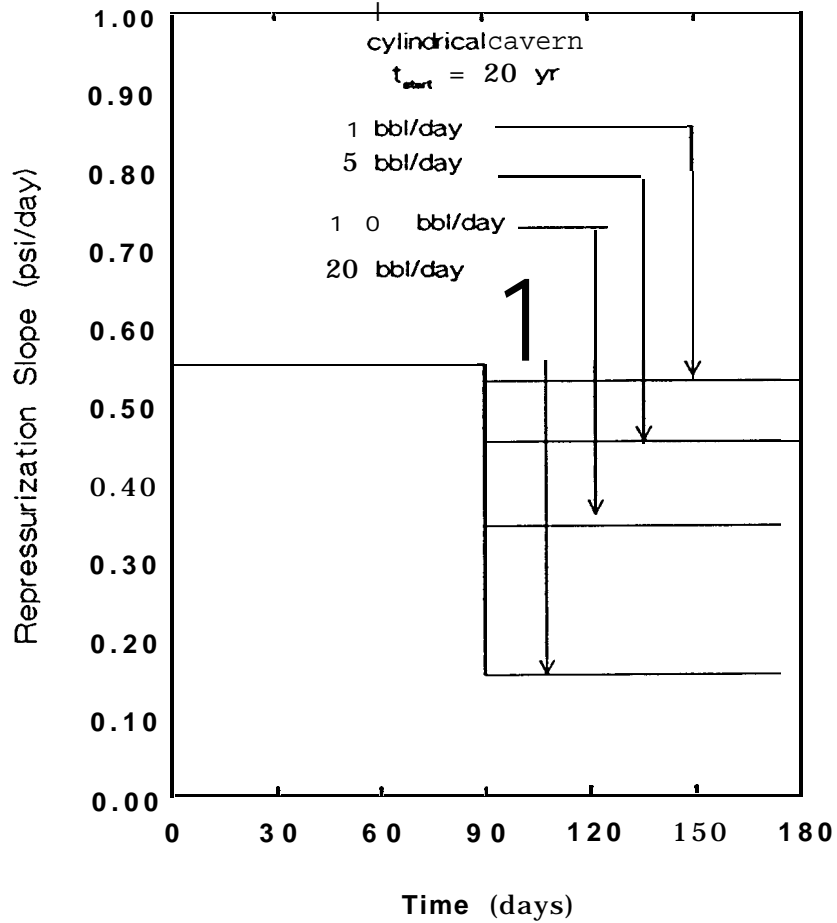


Figure C-3. Repressurization slope for a 2000 - 4000 ft cavern, 20 years after fill, operated at 600 psia, as a function of time, with a 1, 5, 10, or 20 bbl/day leak (from top to bottom in figure), occurring at 90 days.

Distribution:

US DOE SPR **PMO** (4)

900 Commerce Road East

New Orleans, LA 70123

Attn: TDCS (2)

E. E. Chapple

D. W. Whittington

US DOE SPR **PMO** (3)

1000 Independence Avenue SW

Washington, DC 20585

Attn: D. Johnson

D. Smith

H. Giles

Boeing Petroleum Services, Inc. (3)

850 S. Clearview Parkway

New Orleans, La 70123

K. E. Mills

K. D. Wynn

T. Eyennann

NIPER

CORE Labs

Weatherly Labs

SPL Labs

6000 V. L. Dugan
6200 B. W. Marshall
6250 P. J. Hommert
6253 D. S. **Preece**
6257 J. K. Linn (10)
6257 G. S. Heffelfinger (10)
6257 J. T. Neal
6257 J. L. Todd
6257 B. L. Ehgartner
6257 P. S. Kuhlman
1521 R. D. Krieg
3141 S. Landenburger (5)
3145 Document Processing (8)
For **DOE/OST1**
3151 G. C. **Claycomb**
For DOE/TIC
8523 R. C. Christman (Library)